REVIEW ARTICLE

Metallocarbohedrenes: Recent advancements

R. Selvan and T. Pradeep*

Department of Chemistry and Regional Sophisticated Instrumentation Centre, Indian Institute of Technology, Chennai 600 036, India

The recently discovered family of molecular clusters, metallocarbohedrenes (metcars), have generated considerable excitement in cluster chemistry. Metcar research has spread into a large number of transition metals and mixed metals and recent investigations point to the complexity and variety of metcar chemistry. The structure and electronic properties are vigorously studied by various methods of theory. Many of the earlier assumptions have been proved wrong by carefully planned experiments and detailed computational studies. Metcar research will certainly intensify in the years to come in view of their predicted novel properties.

SOME of the most interesting experiments in contemporary chemistry are centered around molecular clusters. Clusters are aggregates of ions, atoms or molecules that are weakly bound together, having properties in-between those of gaseous and condensed states of matter[1]. Most of the available chemistry of molecular clusters is investigated by mass spectrometry. The discovery of buckminsterfullerene[2] in mass spectrometric experiments has added greater impetus to molecular cluster chemistry; the associated physics and materials science also attracted attention. Recently the observation of a peak at 528 amu in the mass spectrum of a laser evaporation experiment culminated in the discovery of yet another class of cage-like molecules called metallocarbohedrenes, shortly 'metcars'[3]. Castleman and co-workers made this discovery while studying the dehydrogenation reaction of hydrocarbons using metal ions, atoms and clusters[3]. The experimental setup they employed for this discovery was a mass spectrometry/mass spectrometry (MS/MS) system coupled with a laser vapourization source. By performing isotopic labelling experiments and reactions with NH_3, they came to the conclusion that the elemental composition corresponding to 528 amu is Ti_8C_{12}. They proposed a pentagonal dodecahedron structure to explain its stability (Figure 1 *a*). They later extended the investigations to other early transition metals[4], V, Zr and Hf and obtained clusters of the same composition, $M_8C_{12}^+$. In the case of Zr there is also multicage formation[5]. Pilgrim and Duncan[6] showed that metcar is also possible with Cr, Mo and Fe; face-centered cubic (fcc) structures beyond metcars (which exists in the cubic form) called nanocrystals[7–10] were also observed. Binary metal metcars of Ti, Y, Nb, Mo, Ta and W have been produced by direct laser vaporization of mixtures of the metal carbide and the metal[11]. Studies related to the mechanism of formation suggest that metal–carbon clusters first develop through multiple ring structures via the successive addition of MC_2 units[12,13]. Photodissociation and metastable decomposition experiments were performed on metcars[7–10] and it was found that the decomposition channel for $Ti_8C_{12}^+$ is through the loss of Ti atom. Castleman *et al.* studied the reaction of metcar with H_2O, NH_3 and CH_3OH which resulted in the formation[14] of $M_8C_{12}(H_2O)_8$, etc. With π-bonding molecules such as benzene it resulted in the formation of M_8C_{12} (benzene)$_4$. Reaction of metcar with acetone is an association process whereas abstraction takes place with iodine to form M_8C_{12}-I (ref. 15). The metcar research until early 1995 was summarized in an earlier review[16]. Since then, many new experiments have been performed and our understanding of these unusual clusters has improved substantially and many of the earlier assumptions have been proved to be untrue. We present here the state-of-the art of the subject matter.

Theoretical investigations on metcars focused mainly on the structure and stability of the cluster. Castleman *et al.* proposed a dodecahedral structure (T_h point group) for metcars[3]. It can be viewed as a cubic M_8 cluster with six C_2 units capping the six faces of the cube[17–30] (Figure 1 *a*). Hay subsequently showed that the electronic configuration with lowest energy for the T_h cage of Ti_8C_{12} corresponds to a nonet state with one unpaired electron each localized on the Ti atoms[31]. Calculations predicted that Ti_8C_{12} with T_h symmetry will undergo Jahn–Teller distortion[32–34]. Another structure which has received considerable theoretical attention with less experimental evidence is the tetracapped tedrahedron of T_d symmetry (and the closely related structure of D_{2d} symmetry), proposed by Dance[35] (Figure 1 *b*). Geometrical optimizations carried out using either density functional approach or *ab-initio* Hartree–Fock methodology show that a 45° rotation of all dicarbon fragments with respect to the underlying skeleton of metal atoms leads to a cage structure with 36 metal–carbon bonds which is much more stable than the pentagonal dodecahedron[35–40].

*For correspondence. (email:pradeep@iitm.ernet.in)

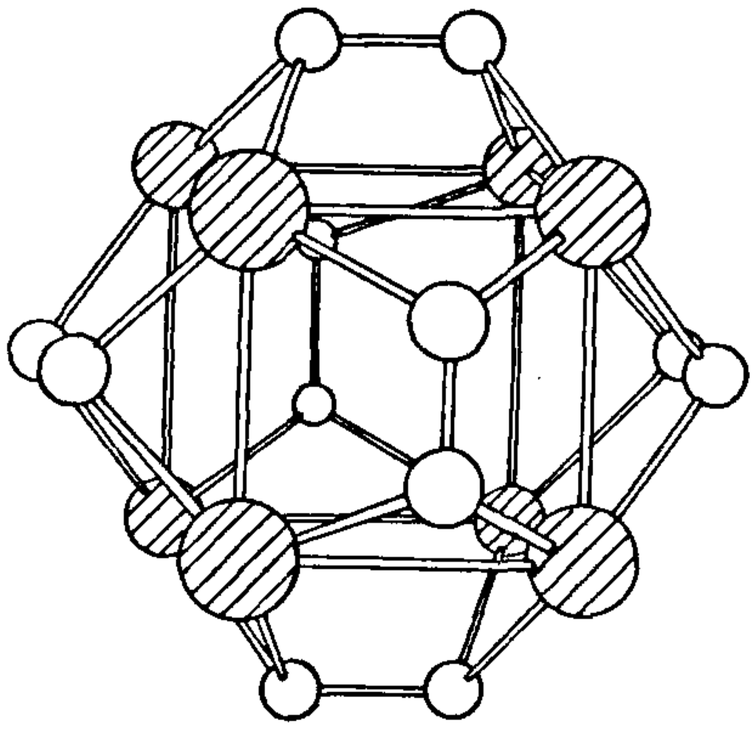

(*a*)

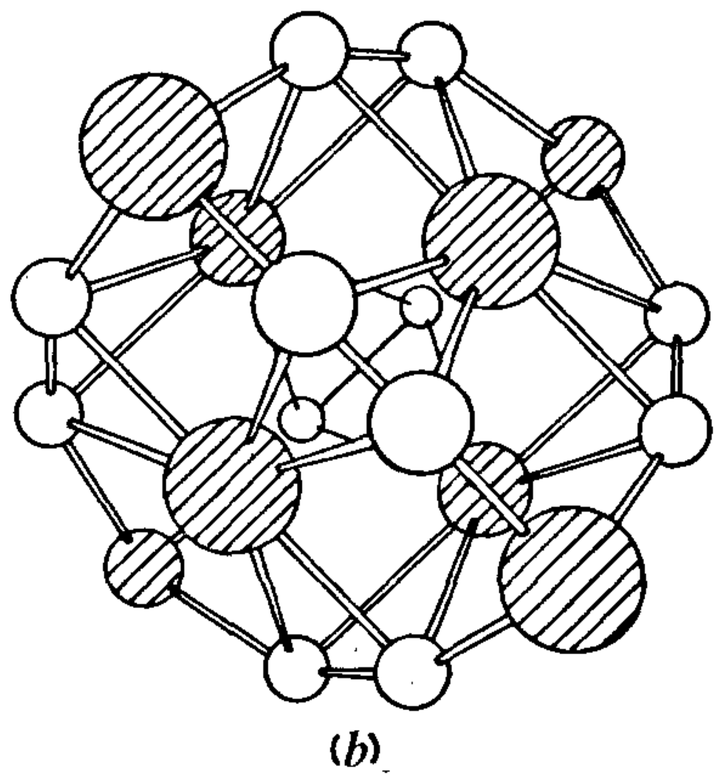

(*b*)

Figure 1. *a*, T_h structure (from ref. 35); *b*, T_d structure (from ref. 35). The open circles denote carbon and the shaded circles denote the metal atoms.

New synthetic approaches towards the production of metallocarbohedrenes

In the beginning, metcars were produced in time of flight mass spectrometers coupled with laser vaporization source[3]. Duncan's group also followed a similar procedure and analysed metcars formed by means of reflectron mass spectrometry[6]. Bowers and coworkers used an ion chromatography apparatus with laser desorption[41]. In all these experiments, dehydrogenation of hydrocarbons by means of metal ions resulted in the formation of metcars. Metcars of Ti and Zr have also been formed by direct laser vapourization of the respective carbides[42]. Binary metal metcars of Ti with Y, Nb, Mo, Ta, and W have been produced by direct laser vapourization of a mixture of Ti carbide and the metal[11]. Later experiments with titanium–graphite mixed rods exhibited the same kind of cluster distribution as was seen with the metal and hydrocarbon[43]. Metcar was also detected in soot obtained by arc evaporation of a Ti–C composite[44]. Recently Lu *et al.* generated metal–carbon clusters from a pulsed arc cluster ion source[45]. Here the pulsed arc cluster ion source is coupled to a reflectron time of flight mass spectrometer. Between two electrically isolated electrodes, a high voltage (up to 1200 V)/high current pulsed arc discharge is fired on the arrival of He gas. The plasma carried by helium travels through a 1.5 mm diameter and 15 mm long channel and supersonically expands into vacuum. In this channel cluster growth takes place. Then the cluster ions cooled by supersonic expansion are carried to the extraction region of a reflectron time of flight mass spectrometer where they are analysed. In this setup, a composite rod prepared by packing a metal oxide/graphite mixture placed within a graphite rod serves as the cathode. Arc evaporation resulted in a mass distribution corresponding to $V_8C_{12}^+$ metcar when the metal oxide is V_2O_5.

Tast *et al.* observed metallocarbohedrenes by the destruction of metal–fullerene clusters[46]. The cluster source they used for this purpose is a low-pressure, inert gas condensation cell. Using a Nd:YAG laser, transition metals were evaporated inside the condensation cell. Fullerene vapour obtained from a resistively heated oven is allowed to mix with the vaporized metals. This vapour mixture is quenched in a low-pressure helium atmosphere cooled by liquid nitrogen. By varying the temperature of the fullerene oven and the power of the vapourization laser, formation of the clusters is controlled. The composition $C_{60}M_x$ and $C_{70}M_x$ formed is carried from the condenzation cell through a nozzle and differential pumping stage into a high vacuum chamber where it is photoionized and mass analysed in a time of flight mass spectrometer. When the reaction was performed between C_{60} and vanadium, it results in a distribution of clusters, $C_{60}V_x$ at lower laser intensities. At higher laser intensities, V_8C_{12} is formed, maybe because of photofragmentation of metal-coated fullerene molecules[46]. Products obtained from the photofragmentation of either $C_{60}V_x$ or $C_{70}V_x$ results in the same distribution of metal carbon clusters with enhancement in the signal for V_8C_{12} cluster. This suggests that V_nC_m clusters produced by the photofragmentation of vanadium-coated fullerenes have no memory of their origin. Similarly, in the case of Ti at low-laser intensities, only $C_{60}Ti_x$ or $C_{70}Ti_x$ are observed, which on exposure to high-laser intensities results in Ti_8C_{12}. In the case of $C_{60}Nb_x$ and $C_{60}Ta_x$, fragmentation behaviour is different from that of $C_{60}V_x$ and $C_{60}Ti_x$. At high-laser intensities, both $C_{60}Nb_x$ and $C_{60}Ta_x$ yield Nb_nC_m and Ta_nC_m respectively with a metal–carbon ratio of 1:1. Fragmentation of $C_{60}V_x$ starts with metal atom loss but in the case of $C_{60}Ta_x$ it starts with carbon loss.

Theoretical studies on metcars

Arriving at the preferred structure of M_8C_{12} computationally is a difficult problem[38], because, it is difficult to

guess the electronic configuration of lowest energy for a given geometry; number of local minima occur on the potential energy hyper surface at the single configuration Hartree–Fock (HF) level and delocalization of metal *d* electrons may alter the results obtained at single configuration HF level[38]. Relaxing the symmetry constraints of T_h point group induces considerable decrease in energy (–350 kcal/mol)[36]. The structure obtained had T_d symmetry and is described as a tetracapped tetrahedron of metal atoms bridged by six C_2 fragments (Figure 1 *b*). Each of the four capping metal atoms (designated as outer metal atoms) are sigma coordinated to three adjacent C_2 units. Each of the inner Ti atoms are surrounded in a planar conformation of six carbons displaying side-on coordination. Calculations by Rohmer *et al.*[38] indicate that the configuration $1a_1^2\ 1t_2^6\ 1e^4\ 1t_1^6\ 2a_1^2$ is not the stable one (previously considered to be stable by Lin and Hall[17,18]). The configuration (considering only 20 metal electrons, see later) corresponds to that of the metal electrons; it is assumed that of the total 32 metal valence electrons, 12 are donated to the six C_2 units and the remaining 20 are distributed in the various molecular orbitals (MOs). The reason for this instability is the symmetry-imposed delocalization of the *d* electrons. The four electrons occupied in orbitals $1a_1$ and $2a_1$ should be localized on specific metal centres. The first possibility is localizing four electrons on the four equivalent metal atoms of the inner tetrahedron resulting in a $^5A_2$ configuration ($1t_2^6, 1e^4, 1t_1^6, 1a_1^1, 2t_2^3$) whereas the other 16 electrons are localized on the other metal atoms. Energy of this structure works out to be –7228.3947 a.u. The second possibility requires the localization of four electrons on four equivalent atoms of the outer tetrahedron, the four MOs equally populated are $2a_1$ and $3t_2$ which give an energy of –7228.22687 a.u., 104 kcal/mol higher than the ground state energy.

Ti_8C_{12} could be mixed valent!

In the quintet ground state[38], metal electrons are localized primarily on four titanium atoms of the large tetrahedron (designated as THN), each having an electronic configuration d^4 and an oxidation state Ti(0). Therefore, sixteen electrons localize on four Ti atoms of the large tetrahedron and the remaining four electrons localize on four outer metal atoms (designated as thn) with electronic configuration d^1 and oxidation state Ti(111). In the excited quintet state, there will be an opposite distribution of twenty electrons among the eight metal atoms. The transition can be represented as,

$$\underset{\text{ground state quintet}}{Ti_4(0)_{THN}\ Ti_4(111)_{thn}} \rightarrow \underset{\text{exited state quintet}}{Ti_4(111)_{THN}\ Ti_4(0)_{thn}}.$$

Geometry of the cage cluster intermediate between these quintets corresponds to the structure of pentagonal

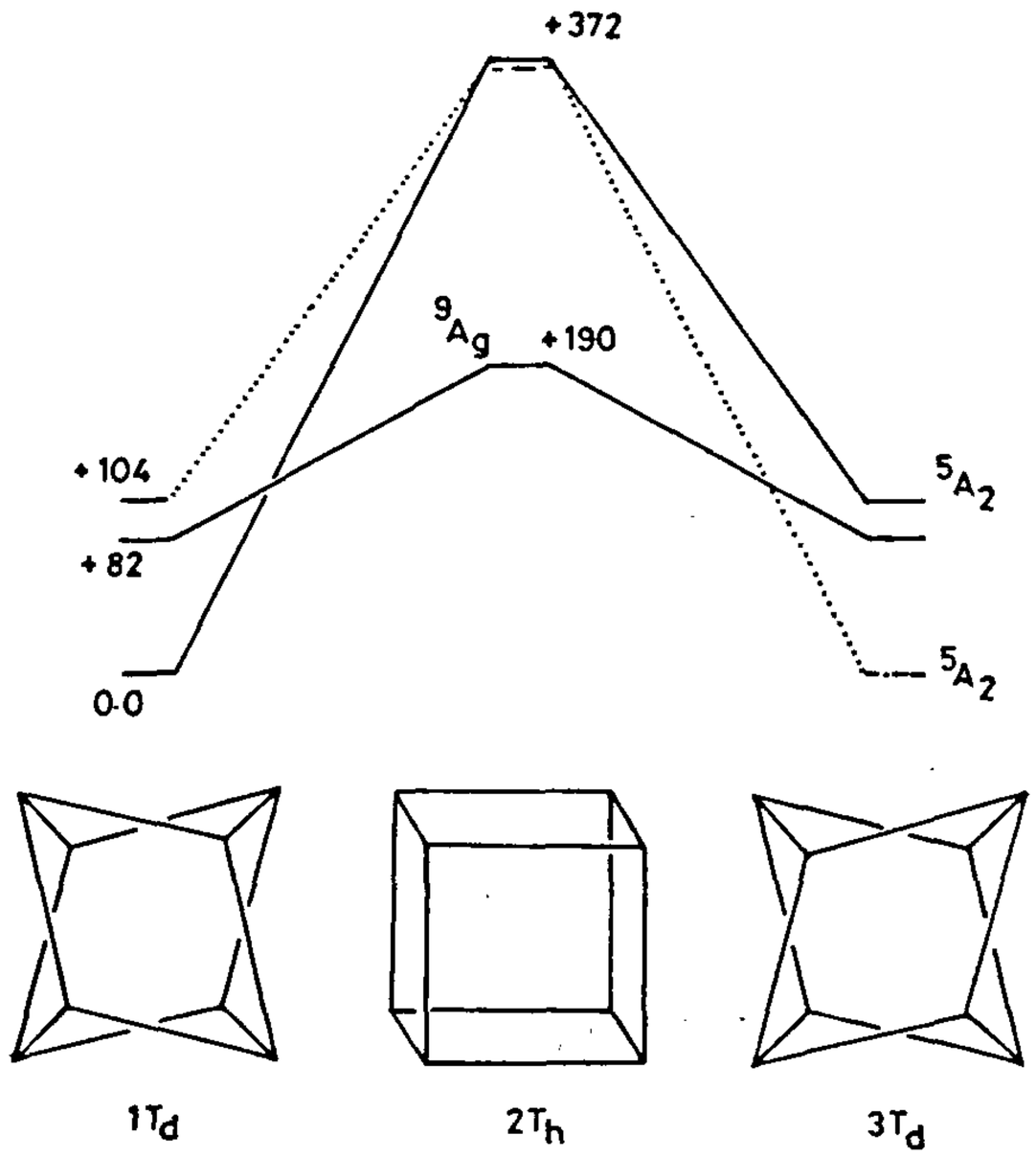

Figure 2. Energy profile computed for a hypothetical interconversion from ground state quintet of T_d form (1) to excited state quintet of T_d form (3) through an intermediate structure with T_h symmetry (2) (from ref. 38).

dodecahedron with T_h symmetry[38]. Self-consistent field (SCF) energy computed for the doubly degenerate quintet state of the T_h structure is –7227.7988 a.u., considerably greater than the energies of the T_d quintet states. Structures and energetics of the transition are shown in Figure 2 where the structures are denoted as **1**, **2** and **3**. This large barrier for conversion is due to Ti–C interaction being less favourable in **2**. In **1** and **3**, the dicarbon units are part of a planar, acetylene-like Ti–C≡C–Ti structure. The electronic structure of acetylenic molecules is retained in the quintet state of 2 even though the Ti–C≡C–Ti skeleton is not planar any more. The T_h structure has an ethylenic structure. Apart from T_d, other structures do exist on the potential energy hyper surface[35]. A singlet coupling of four unpaired electrons in T_d symmetry leads to the lower energy $^1A_1$ state and the quintet $^5A_2$ state is higher in energy by 6.5 kcal/mol, in a configuration interaction (CI) calculation[38]. This distinctive stability of T_d structure is due to specific arrangement of C_2 ligands which separates sigma interactions involving the large tetrahedron of metal atom from π-interactions in the small tetrahedron. In the singlet state, Ti–Ti distance was decreased in thn (3.052 Å) with respect to the quintet state (3.114 Å) (ref. 39). Triplet coupling of four electrons leads to a low energy $^3T_1$ state[39]. The singlet–triplet energy gap is

2.4 kcal/mol at the SCF level and 2.9 kcal/mol at the CI level[39]. Transferring the localization site of four unpaired electrons from thn to THN results in a series of states. This results in expansion of the small tetrahedron and increase in bond distances except for C–C. This geometrical change is due to electrostatic repulsion induced by four unpaired electrons toward the metal atoms of the other tetrahedron.

Electronic structure of metallocarbohedrenes

Electron localization appears to be an important issue in the assignment of the ground state of metcars. Hay investigated Ti_8C_{12}, considering it to have T_h symmetry and found that Ti atoms are too far apart to generate an antiferromagnetic coupling so that the nonet state is more stable[31]. According to him, eight metal electrons are localized on eight equivalent titanium atoms. But in the T_d structure, there are two subsets of metal atoms (THN) and (thn). Each C_2 fragment is sigma-bonded to two metal atoms of THN and is acetylenic type, considered as C_2^{2-}. The number of metal electrons in the cluster is therefore 32 – 12 = 20. Sixteen metal electrons are in eight MOs ($1t_2 + 1e + 1t_1$) which take an active part in back donation towards π^* orbitals of the C_2 units. The problem of localization/delocalization starts from the remaining four electrons. Four electrons can be localized either on thn or THN, both are quintet states separated by 104 kcal/mol. Stable quintet is the one in which four electrons are localized on thn. This configuration is favoured, because of the occupation of the MO $1a_1$ (a bonding combination); here dz^2-like orbitals are pointing in-phase towards the small tetrahedron located 1.91Å from each apex. But in $2a_1$ (bonding combination) the large tetrahedron size prevents overlap between 3d orbitals of Ti. Antiferromagnetic coupling of four unpaired electrons induced by relative stability of $1a_1$ with respect to $2t_2$ accounts for the singlet ground state. Energy stabilization due to the coupling of four unpaired electrons was computed to be $E_s/q = 6.5$ kcal/mol with respect to the quintet state. Ground state of Ti_8C_{12} corresponds to localization of four unpaired electrons on four metal atoms of thn site. Because of short Ti–Ti distances in thn, an antiferromagnetic coupling develops through in-phase combination of four dz^2-like orbitals ($1a^1$ bonding orbital) and the ground state[39] is $^1A_1$.

Ian Dance in his calculations has shown that there is a barrierless transformation of Ti_8C_{12} from isomer T_h to T_d with the consequence that even metastable occurrence of T_h is not possible[40]. The transformation needs an intermediate loss of mirror symmetry. Dance calculated the energy and geometry changes during 33 steps of transformation of Ti_8C_{12}. In first eight steps, there is an energy reduction with twisting of opposite C_2 groups and increase in Ti–Ti distances. Dance has also studied the mechanism of transformation of $Ti_{14}C_{13}$ to Ti_8C_{13} by means of gradient corrected-density-functional method[37]. By optimization of the structures of the intermediates, the mechanism proposed by Pilgrim and Duncan for the sequence of extrusion reactions is supported and substantiated. He has drawn important conclusions from calculating binding energies of $Ti_{14}C_{13}$, $Ti_{13}C_{13}$, $Ti_{12}C_{13}$, $Ti_{11}C_{13}$,$Ti_{10}C_{13}$, Ti_9C_{13} and Ti_8C_{13}. They are: (i) the first stage of photoextrusion of Ti from $Ti_{14}C_{13}$ must be unfavourable thermodynamically, (ii) the second stage (formation of $Ti_{12}C_{13}$ through photoextrusion of Ti from $Ti_{13}C_{13}$) is more favourable, (iii) the intermediate $Ti_{11}C_{13}^{\dagger}$ with three-fold symmetry and with structural features similar to $Ti_8C_{13}^{\dagger}$ is energetically favourable, and (iv) the thermodynamic energy requirements for 4th, 5th and 6th extrusions of Ti atoms are lower than those of the first three.

Arshad Khan proposed a metal-decorated carbon cage structure to explain Duncan's experiments[47]. He calculated the energy to remove the Ti atom from a central position and a corner position to get $Ti_{13}C_{13}$ in the fcc structure proposed by Duncan. It was found that more energy is needed to remove a Ti atom from a central position than from a corner position. The mechanism proposed by Pilgrim and Duncan[48,49] is not in accordance with this observation. In photodissociation experiments, $Ti_{14}C_{13}$ gives Ti_8C_{13}, which suggests that there are six weakly bound Ti atoms in $Ti_{14}C_{13}$. So the antiprism metal decorated carbon (MDC) cage structure was proposed, with an extra carbon atom within the cavity and six Ti atoms bonded around the hexagonal plane of carbon atoms. This structure has six weakly-bound Ti atoms which can readily dissociate to a Ti_8C_{13} structure. From binding energy values calculated, both fcc and D_{3d}(MDC) structures can be valid but fcc fails to explain the experimental results. $V_{14}C_{13}$ gives V_8C_{13}, $Fe_{14}C_{13}$ forms $Fe_{12}C_{12}$ rather than $Fe_{14}C_{12}$ and $Zr_{14}C_{13}$ gives Zr_8C_{12} but not Zr_8C_{13}. All these uncertainties are suggested to be due to the experimental error at high mass numbers (mass error = 1 carbon atom, see below).

Khan has also studied different isomer structures of neutral Ti metcar (Ti_8C_{12}) and compared their stabilities[50]. Binding energy of 6.95 eV/atom for the antiprism MDC structure is larger than most of the distorted decahedron (DD) structures which range from 6.1 to 6.6 eV/atom. So MDC structure is the most favourable structure[50,51]. Isomers studied are the MDC structure, cubic structure and the DD structure. From this MDC structure, Khan was able to explain the photodissociation experiment, mixed metcar formation, etc.[47,51].

Benard *et al.* investigated the addition of NH_3, Cl, CO and C_6H_6 to Ti_8C_{12} by means of *ab-initio* Hartree–Fock and density functional theory calculations[52]. The T_d symmetry structure with two different metal sites, considered to be the more stable one, was chosen for modelling. Addition of four ligands to the external

tetrahedron of metal atoms is found to be exothermic. Formation of $Ti_8C_{12}(Cl)_4$ is highly exothermic. When L = Cl or NH_3, addition of four more ligands to $Ti_8C_{12}(L)_4$ appears to be feasible. In this case, Cl or NH_3 gets easily added to the inner tetrahedron, resulting in the formation of $Ti_8C_{12}(L)_8$. In the case of π-bonding molecules like benzene and weakly polar molecules like CO, only four molecules are added since they have lesser affinity for inner tetrahedron of metal atoms.

Khanna[53] has explored the possibility of formation of mixed metallocarbohedrenes containing metal, carbon and nitrogen. His suggestion was to substitute two C_2 units each at the top and bottom by means of nitrogen molecules leading to $Ti_8N_4C_8$ (ref. 53). From experiments, it is already known that fragmentation of Ti_8C_{12} results in loss of Ti atoms until Ti_4C_{12} is reached followed by carbon cluster losses. Therefore, to open the metcar cage, removing C_2 units is difficult. But in $Ti_4N_4C_8$ weak N–N bond can be broken and endohedral implantation can be done. *Ab-initio* self-consistent calculations carried out assuming a D_{2d} structure show that N–N bond in metcar cage (2.82 a.u.) was larger than that of free nitrogen molecule (2.13 a.u.). Binding energy calculated for the nitrogen molecule in $Ti_8N_4C_8$ is 6.5 eV. Therefore, this cluster should be stable and can be observed in experiments.

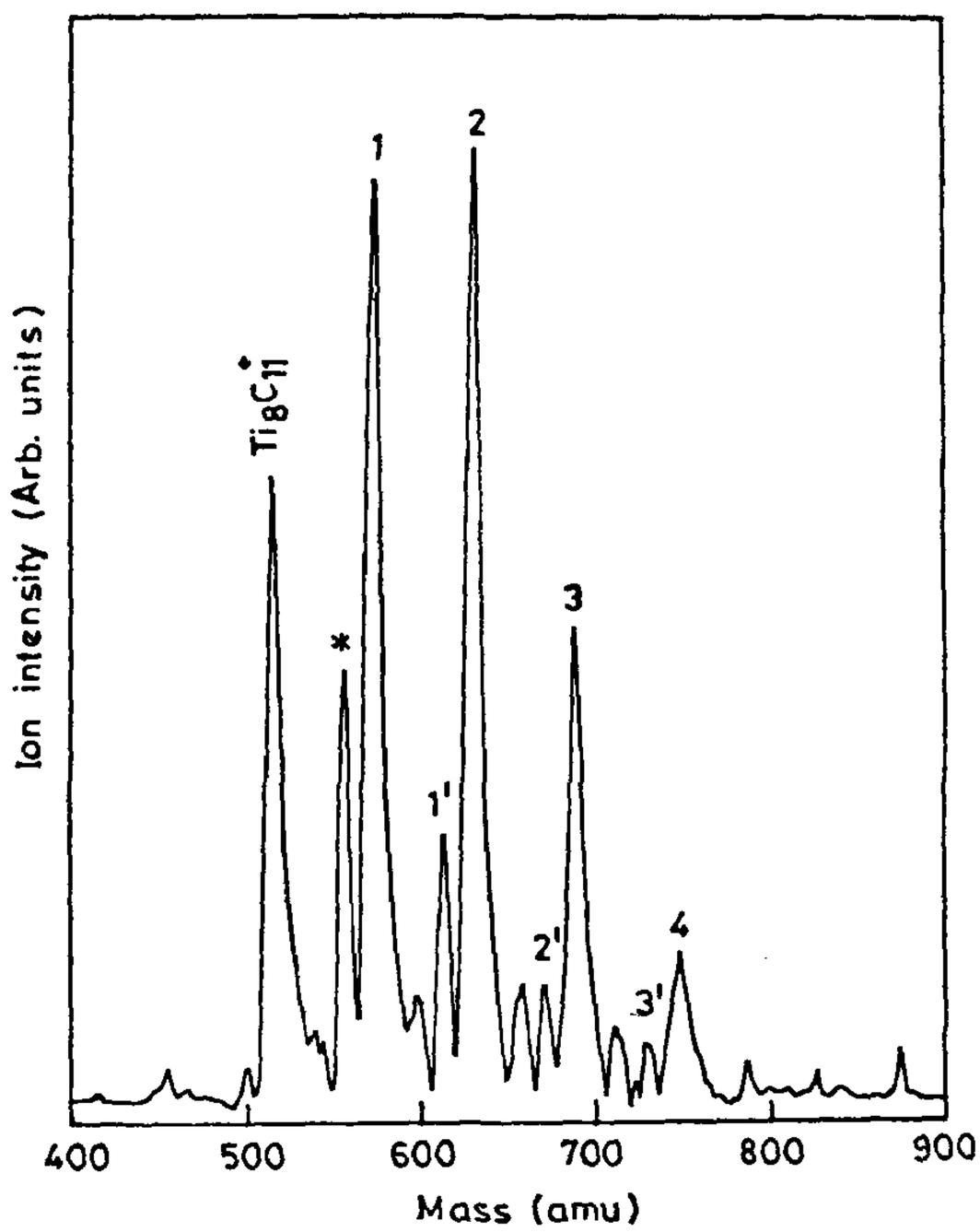

Figure 3. Product distribution arising from multistep reactions of $Ti_8C_{11}^+$ with acetone. The peak labelled by 1 corresponds to the association reaction of $Ti_8C_{11}^+$ with acetone. The peak labelled by * is the chemical reaction product. Association products on to the peaks marked 1 and * are labelled *n* and *n'* respectively (from ref. 54).

Experiments to probe the structure

It is known that $Ti_8C_{12}^+$ reacts with molecules such as H_2O, NH_3, CH_3OH, and C_6H_6 mainly via an association mechanism. To find whether the reactivity of $Ti_8C_{12}^+$ and its stability are similar to other titanium clusters ($Ti_8C_{13}^+$, $Ti_8C_{11}^+$, etc.), reactions of clusters with acetone were examined[54]. As already known, $Ti_8C_{12}^+$ undergoes association reaction with acetone, but $Ti_8C_{11}^+$ exhibits both association reaction and breakage of chemical bonds (Figure 3). These two reactions can be described as,

Association reaction

$$Ti_8C_{11}^+ + CH_3COCH_3 \rightarrow Ti_8C_{11}^+(CH_3COCH_3)$$

Chemical reaction

$$Ti_8C_{11}^+ + CH_3COCH_3 \rightarrow Ti_8C_{11}^+(COCH_3) + CH_3.$$

This result was rationalized in terms of the closed cage structure proposed for metcars. $Ti_8C_{11}^+$ has a vacancy left by the missing carbon atom, which leads to an opening in the cage. When this cluster reacts with acetone, reactant molecule breaks and $COCH_3$ unit from acetone fills the hole left by the missing carbon atom in the cage, so that the cage can be closed. In the case of $Ti_8C_{13}^+$, three possible channels of reaction are found: (i) association reaction, (ii) the dominant pathway leading to $Ti_8C_{12}^+$, i.e. $Ti_8C_{13}^+ + CH_3COCH_3 \rightarrow Ti_8C_{12}^+$ + products, and (iii) replacement reaction, where a carbon atom is replaced by an acetone molecule or its fragment.

$Ti_8C_{14}^+$ also displays reactions similar to that of $Ti_8C_{13}^+$. Both $Ti_8C_{13}^+$ and $Ti_8C_{14}^+$ fragment to $Ti_8C_{12}^+$ by loss of one or two carbon atoms which confirms the proposed closed cage structure for metcar. Reactions exhibited by $Ti_8C_{13}^+$ and $Ti_8C_{14}^+$ are different from $Ti_8C_{11}^+$. Different pathways may be due to the coexistence of several isomeric structures. For example, in the case of $Ti_8C_{13}^+$, the isomer which is more reactive undergoes chemical reaction involving the breakage of bonds. The other isomer which is less reactive (carbon doped metcar) undergoes association reaction. These studies confirm that neighbouring Ti–C clusters are more reactive than the metcar, $Ti_8C_{12}^+$. Lack of reactivity of $Ti_8C_{12}^+$ with CH_3COCH_3 is consistent with a closed shell thermodynamically stable molecular cluster.

Metcar adducts

Metcar adducts $Ti_8C_{12}^+(M)_n$ (M = halogens, π bonding molecules and polar molecules, n = 1–8) are formed by

thermal reactions. Metcar undergoes abstraction reactions with halogens to form $Ti_8C_{12}^+-X + X^\cdot$, association reaction with π bonding molecules (see below) leads to adducts such as $Ti_8C_{12}^+(pyridine)_4$, $Ti_8C_{12}^+(CH_3COCH_3)_4$ and $Ti_8C_{12}^+(CH_3CN)_4$ and polar molecules such as 2-butanol gives a truncation at $Ti_8C_{12}^+(2\text{-butanol})_8$ (ref. 55). By the direct interaction of Ti with mixtures of methane and selected reactant gases, a new method has been developed for the formation of metcar–ligand complexes. Three different types of reactions exhibited by metcars were identified. Oxidation occurs when metcars react with halogen containing molecules through valence electron donation from $Ti_8C_{12}^+$ to the halogen atom. With π bonding molecules, $Ti_8C_{12}^+$ forms 'surface complexes' in which a ligand binds two metal atoms in the pentagonal ring through d–π interaction. So a maximum of four π-bonding molecules are accepted, leading to a truncation at $Ti_8C_{12}^+(\pi\text{-bonding molecule})_4$, this is true with benzene and acetylene. With acetone, pyridine and acetonitrile, product distribution truncates at $Ti_8C_{12}^+(Y)_4$, where Y = acetone, pyridine or CH_3CN. Very small peaks of $Ti_8C_{12}^+(Y)_{5,6}$ are also observed, because these molecules are both π-bonding and polar. It may be concluded that π-bonding molecules associate to $Ti_8C_{12}^+$ differently than non π-bonding molecules do.

In contrast, ion–dipole interaction leads to the formation of $Ti_8C_{12}^+(M)_{1-8}$ where M are polar molecules[55]. With 2-butanol, there is a truncation at $Ti_8C_{12}^+(2\text{-butanol})_8$ which supports the structure proposed by Castleman. According to Castleman, if theoretically predicted T_d structure is correct, then there should either be a prominent cluster distribution or a magic number or truncation at $Ti_8C_{12}^+(\text{polar molecule})_4$, but none has been seen hitherto.

$Ti_8C_{12}^+(I)$ formed from reaction of Ti plasma with a mixture of methane and MeI was mass selected and its reaction with methanol was studied. Here cluster distribution terminates at $Ti_8C_{12}^+(I)(\text{methanol})_7$, which confirms that eight metal atoms in Ti_8C_{12} are reactive and one Ti atom can associate with only one reactant molecule, which is against the T_d structure, suggesting that only four Ti atoms are reactive.

Frieser *et al.*[56,57] studied the reactions of metallocarbohedrene $V_8C_{12}^+$ with H_2O, NH_3, ROH (R = CH_3, C_2H_5, etc.) and CH_3X (where X = Cl, Br and I). Upon the reaction of $V_8C_{12}^+$ with trace quantities of H_2O in an ion cyclotron resonance (ICR) cell, the spectrum obtained showed complex reaction sequences (Figure 4). The reaction proceeds in three steps: (i) initial association of H_2O, (ii) addition of second water molecule leads to the elimination of hydrogen yielding $V_8C_{12}(OH)_2^+$, and (iii) further reaction leads to a truncation at $V_8C_{12}(OH)_2(H_2O)^+$. This final product remains inert even when reaction time and pressure of water were increased to 40 s and 3.9×10^{-8} torr, respectively[57]. With

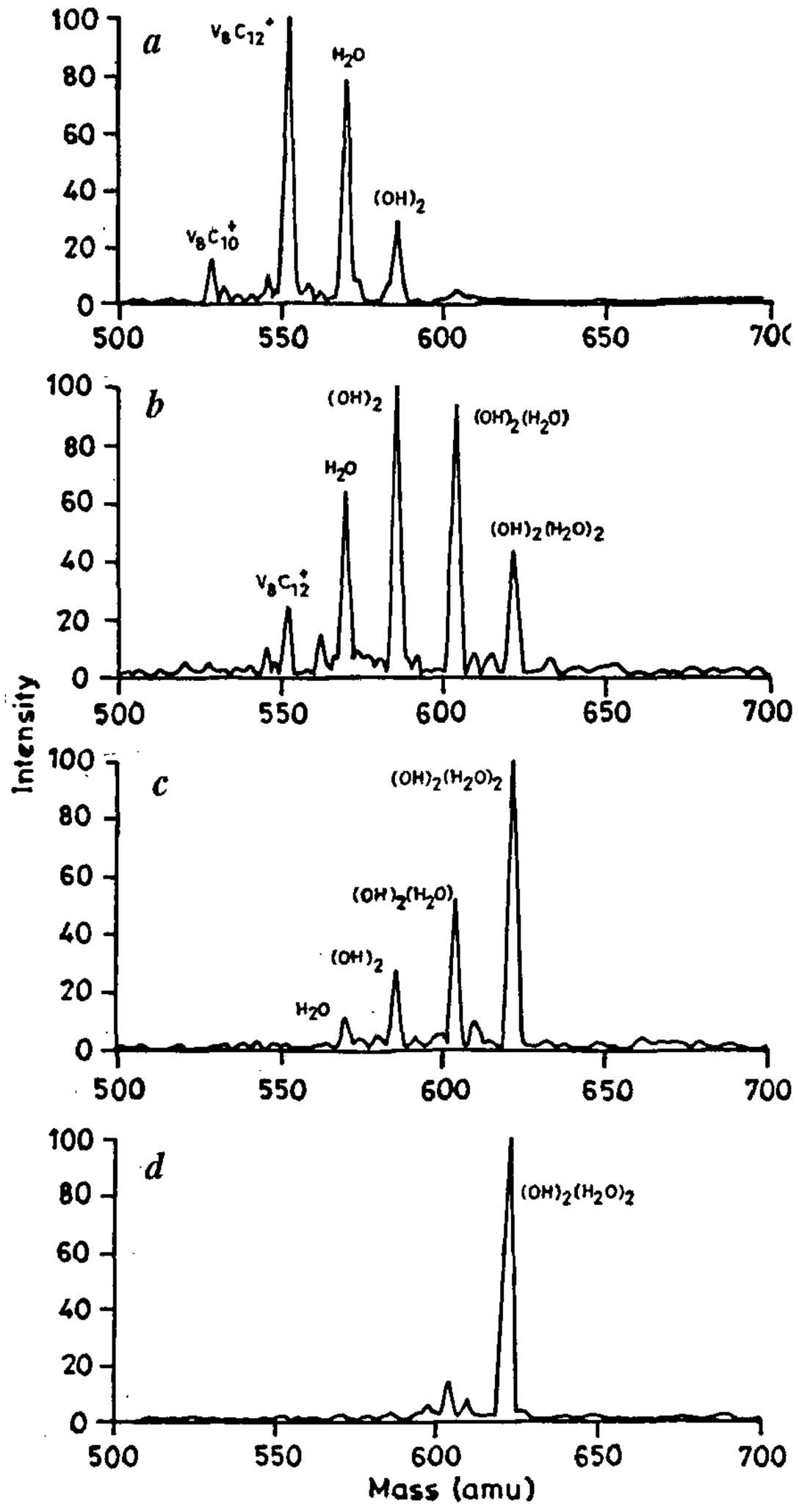

Figure 4. Reaction of $V_8C_{12}^+$ with water at different reaction times. *a*, 2 s; *b*, 6 s; *c*, 10 s and *d*, 14 s (from ref. 57).

NH_3 and alcohols also there is a truncation at $V_8C_{12}(NH_3)_4^+$ and $V_8C_{12}(ROH)_4^+$, respectively. When reaction time was increased to 48 s, $V_8C_{12}(NH_3)_5^+$ peak started appearing. Therefore, the first four reactions of alcohols or NH_3 with $V_8C_{12}^+$ are fast while subsequent reactions are slower. There is no formation of $V_8C_{12}(NH_3)_8^+$ because the experiments were done under lower pressures. $V_8C_{12}^+$ on reaction with CH_3I forms $V_8C_{12}(I)_3^+$, which on further reaction with trace water leads to a truncation at $V_8C_{12}(I)_3(H_2O)^+$. $V_8C_{12}(I)_3(H_2O)^+$ is unreactive with water and CH_3I, suggesting that unpaired electrons are not equally delocal-

ized over the eight metals[57]. In reaction of $V_8C_{12}^+$ with both polar and π-bonding ligands, there is a truncation observed after attaching four ligands. When additional ligands are added, they add more slowly and take longer time than the first four for the process to occur. These results are in favour of the theoretically proposed T_d or D_{2d} structure.

However, in studies of $Ti_8C_{12}^+$ with 2-butanol, Castleman *et al.*[55] saw eight attachments at same rate with no formation of $Ti_8C_{12}L_4^+$ (where L is the ligand). This suggests that reactivity and geometry of $V_8C_{12}^+$ are quite different from that of $Ti_8C_{12}^+$. Byun and Frieser *et al.*[57] have done these studies in an FT–ICR spectrometer at low pressure to distinguish strong binding sites on the cluster. But in Castleman's experiments[55], even though metal sites are not equivalent, all the eight ligands can bind with sufficient energy to be stabilized by subsequent collisions.

An important conclusion from these studies concerns with the number of unpaired electrons the clusters have which make their reactivity different[57]. For example, $Ti_8C_{12}^+$ has one unpaired electron and there is no dehydrogenation reaction with H_2O but it abstracts one iodine, $V_8C_{12}^+$ has four unpaired electrons so one dehydrogenation reaction and four iodine abstractions are observed and $Nb_8C_{12}^+$ has five unpaired electrons so two dehydrogenations and five iodine abstractions are seen. All $M_8C_{12}^+$ (M = Ti, V and Nb) clusters have more than one degenerate highest occupied molecular orbitals. There are odd number of unpaired electrons and therefore these clusters distort to achieve a stable geometric structure from T_h to T_d (or) D_{2d}.

Frieser *et al.*[58] have also studied the gas phase reactivities of $V_{14}C_{12}^+$ and $V_{14}C_{13}^+$, both of them are found to react with H_2O via a combination of association reactions and H_2 eliminations. Loss of H_2 occurs once and twice to form $(OH)_2$ and $(OH)_4$, respectively for $V_{14}C_{13}^+$ while only $(OH)_2$ adducts are observed for $V_{14}C_{12}^+$. With acetonitrile, both the ions undergo only addition reaction. All reactions with H_2O and CH_3CN truncate sharply at eight attached ligands. These results for $V_{14}C_{12}^+$ and $V_{14}C_{13}^+$ are consistent with the behaviour of cubic structure, in which eight metal atoms in the corners are the active binding sites.

Frieser *et al.*[59] have also generated $Nb_8C_{12}^+$ with the same instrument and studied its reaction with H_2O, NH_3, ROH, CH_3CN, RI, etc. where $R = CH_3$. With H_2O, $Nb_8C_{12}^+(H_2O)$ gets formed which reacts with a second molecule of water to eliminate H_2 and results in $Nb_8C_{12}^+(OH)_2^+$. This further reacts and subsequent reaction truncates at $Nb_8C_{12}(OH)_4^+$. There is no further reaction even after 40 s and high pressures of $\sim 1.7\times 10^{-7}$ torr (ref. 48). With NH_3, $Nb_8C_{12}(NH_3)_4^+$ was formed first and as the reaction time was increased to 45 s, higher order peaks $Nb_8C_{12}(NH_3)_5^+$ and $Nb_8C_{12}(NH_3)_6^+$ were observed to grow slowly. These results agree with the prediction of Dance[36]. Lin and Hall[18] expected that four outer metal atoms have larger open coordinate sites which result in the first four fast reactions, while the four inner metals bind ligands less strongly because they are blocked or less exposed to incoming ligands. In case of alcohols, truncation is observed at $Nb_8C_{12}(OR)_4^+$, the formation is less pronounced going from water to methanol to butanol. These trends observed with $V_8C_{12}^+$ are attributed to the increased degrees of freedom afforded by larger alcohols. With acetonitrile and benzene also, similar truncation was observed at $Nb_8C_{12}(CH_3CN)_{1\text{-}4}(H_2O)^+$ and $Nb_8C_{12}(C_6H_6)_4^+$ which is consistent with the distorted metcar structure. Castleman's suggestion that ligands π-bond to two metal atoms in each of the four pentagonal faces is problematic for benzene, where nonbonded carbons could interact unfavourably causing rearrangement and loss of aromatic stabilization of benzene[59]. To further eliminate this possibility, $Nb_4C_4^+$ and $Nb_6C_7^+$ were allowed to react with CH_3CN and benzene. No truncation was observed at $Nb_4C_4L_4^+$, which is against Castleman's explanation. Therefore, each benzene or CH_3CN coordinates to one metal atom and not to two metal atoms.

Sequential halide abstraction with CH_3X yields $Nb_8C_{12}X_n^+$ truncating at $n = 4$ for X = Cl and $n = 5$ for X = Br and I. $Nb_8C_{12}(I)_4^+$ is formed quickly, but $Nb_8C_{12}(I)_5^+$ forms very slowly. This is because $Nb_8C_{12}^+$ has five unpaired electrons out of which four electrons are localized on four outer metals in a distorted structure, which results in four fast halide abstractions. The remaining one electron could be localized on four inner metals which are involved in one or more slower halide abstractions. So the titration results and the relative rate constants for the sequential addition reactions of NH_3 provide supportive evidence that geometric structure of $Nb_8C_{12}^+$ is the theoretically more stable T_d or D_{2d} one having two sets of four equivalent metal sites, as opposed to T_h symmetry with all eight equivalent metal atoms. Again all these discrepancies between reactivity of $Nb_8C_{12}^+$ and $Ti_8C_{12}^+$ may be due to the number of unpaired electrons. In general, in all of the four reactions studied, the first four reactions with $Nb_8C_{12}^+$ were observed to be fast, leading to a build-up or truncation of the complex with four ligands attached. Further reactions are slower than the first four. These results support distorted structures. In contrast, Castleman *et al.*[55] saw eight attachments to $Ti_8C_{12}^+$ at same rate with no build-up of $Ti_8C_{12}L_4$ with 2-butanol, which is in favour of the T_h structure. Based on abstraction of iodine from CH_3I, the number of unpaired electrons on Nb_8C_{12} and Ti_8C_{12} may be five and one, respectively.

Thus with different valence electrons, with different number of unpaired electrons, and with different diffusive characteristics, it is reasonable that $Nb_8C_{12}^+$ and $Ti_8C_{12}^+$ might have different structures.

Ion chromatography (IC) in the gas phase

Here the ion source is composed of a laser desorption supersonic expansion apparatus which creates intense cluster beams[60]. The chromatography cell is the most important part of the experimental set-up. Here mass-selected ions are injected through a small hole at low energies (1 to 5 eV in the laboratory frame of reference, < 0.1 eV centre of mass) into the cell filled with 2 to 5 torr of He, with a small amount of reactant gas, at 10^{-4} to 10^{-5} torr partial pressure. The ions are rapidly thermalized when they enter the cell. They drift through the cell under the influence of the weak electric field (1–10 V/cm) in t_d = 100-1000 μs, and experience 10^4 to 10^5 collisions with He[60,61]. The time for the ions to traverse the cell depends on their mobility, which in turn depends inversely on the collision cross section of the species with He gas. Larger the cross section, smaller the mobility and longer the time. The drift velocity is,

$$V_d = Z/t_d, \tag{1}$$

where Z is the cell length and it is the mobility $K = A/\sigma$ where σ is the collision cross section and A is a constant which includes mass, charge and temperature. For ions of fixed mass,

$$t_d = Z\sigma/AE. \tag{2}$$

From (2) the time the ions spend in the chromatography cell is proportional to collisional cross section of that ion with the gas. Thus for two different species having the same mass,

$$t_d(1) = \sigma(1)/\sigma(2)t_d(2) \tag{3a}$$

$$t_d(1) - t_d(2) = Z/AE\ \{\sigma\ (1) - \sigma\ (2)\}, \tag{3b}$$

[1] and [2] refer to ion types. If a very short pulse of ions is subjected into the cell, ions with different structures will exit at different times, even if they have the same mass. So, by measuring the mobility of the cluster ions using ion chromatography experiment, shape of the same can be probed. Ions drift through helium to the quadrupole mass filter and reach the detector where an arrival time distribution (ATD) is obtained. For a cluster ion with a single geometric isomer, the ATD could be converted to an ionic mobility. In case of multiple isomeric structures, ATD would have several peaks and so IC device would separate them if they differ in shape. Using this technique, Bowers *et al.* studied the mobilities of $Ti_8C_{12}^+$, $Ti_8C_{13}^+$, $Ti_8C_{11}^+$, etc. Arrival time distribution obtained[62] for $Ti_8C_{12}^+$ (mobility = 5.78 cm^2 $V^{-1}s^{-1}$) agrees well with the theoretically-predicted shape (mobility = 5.71 cm^2 $V^{-1}s^{-1}$). After choosing a structure (T_h or distorted dodecahedron or cubic), Monte Carlo methods were used to obtain its cross section for collision with He and subsequently theoretical ionic mobility was obtained. By this study, Bowers *et al.* found that T_h structure proposed by Castleman fits well with the predicted ionic mobility. There is a slight deviation for distorted dodecahedron structure whereas the possibility of cubic can be ignored for it has a large deviation. They have also studied the growth mechanism of $Ti_8C_{12}^+$ by injecting it into the IC cell at high energy which results in the formation of $Ti_7C_{12}^+$ with the loss of Ti atoms. This is in agreement with photodissociation experiment of Pilgrim and Duncan[48]. Theoretical mobility of $Ti_7C_{12}^+$ also agrees with experiment which proves that it has a cage structure. They have also generated $Ti_8C_{13}^+$ and its mobility was found to match with the structure in which a carbon atom is attached to $Ti_8C_{12}^+$ (an exohedral species). But Pilgrim and Duncan predicted that $Ti_8C_{13}^+$ formed from photodissociation of $Ti_{14}C_{13}^+$ is an endohedral species. Therefore, $Ti_8C_{13}^+$ produced in IC experiment and the one formed in photodissociation experiment could be two different isomers.

Castleman *et al.* have also probed the structure and stability of metcars by producing mixed metcars in the gas phase. Vapourization of Ti and graphite in the molar mixture ratio of 1:1, 4:1 and 6:1 shows that metcar (Ti_8C_{12}) intensity is increased as the concentration of Ti in the mixture is increased. In this experiment, Castleman *et al.* did not observe the formation of C_{12}, TiC_2, Ti_2C_{12}, etc. So the mechanism proposed by Khan[50], i.e., the formation of C_{12} cage followed by the addition of metal atom, is incorrect. Vapourization of Ti–C and Zr in the molar ratio of 2:1, 4:1, 8:1 and 12:1 yielded $Ti_xZr_y(x + y = 8)$ (Figure 5). If tetracapped tetrahedron

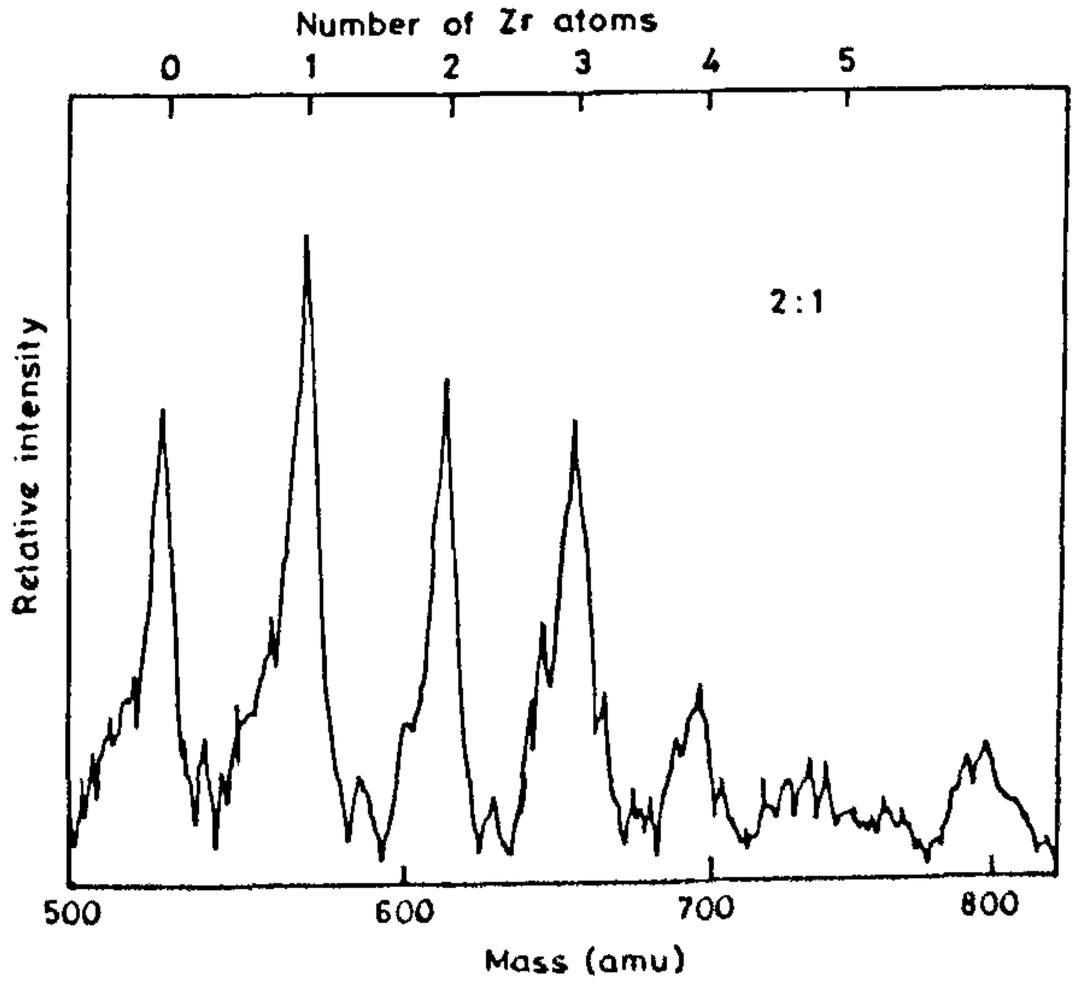

Figure 5. Mass spectra of $Ti_xZr_yC_{12}^+$ under direct laser vapourization conditions with 2:1 molar ratio of titanium and zirconium (from ref. 63)

structure is correct, then $Ti_4Zr_4C_{12}$ should be stable. But $Ti_6Zr_3C_{12}$ and $Ti_3Zr_5C_{12}$ are also observed to be stable[63]. This confirms that the metal sites in the cluster are equivalent. Metcar is more stable in the case of Ti atoms and is less stable with IIIA and VA group metals. In metal carbon bonding, a vacant orbital can accept electrons from the ligand. Metal–carbon bonding is strengthened by back donation (by a synergic process in which low-lying π^* orbitals of the C_2 units accept electrons from metal *d* orbitals which strengthens the metal–carbon sigma bond). In the case of yttrium there is no back bonding, possibly because its electropositive nature precludes the donation of electrons into metal orbital and also due to the absence of metal electron to be donated to vacant π^* orbitals of C_2 units. So Y–C bonds are unstable. Vanadium can accept electrons from C_2 units but destabilizes C_2 by back donating two valence electrons to π^* antibonding orbitals. Nb and Ta metcars are unstable because they easily form metal–metal bonds. Electropositive nature of IVA metals is less than IIIA but more than VA. The d^4 configuration favours 3 M–C sigma bonds, with one remaining electron forming back bond. Because of these reasons, Ti is found to be the suitable metal for metcar formation since Zr and Hf form metal–metal bonds.

To acquire more information about metcars as new electronic, optical and catalytic materials, oxidation reaction of metcar was investigated by Castleman *et al.*[64]. Vapourization of Ti in the presence of methane and He results in the formation of both neutral and ionized clusters. Using a quadrupole filter, cluster ions were excluded and neutrals were allowed to react with oxygen leading to the formation of $Ti_8C_{12}^+$. These neutrals on reaction with other gases like NO_2, CO, etc. do not yield $Ti_8C_{12}^+$. Changing the carrier gas from He to Ar or N_2 does not affect the ionization of the neutral. Only oxygen plays a role in the ionization of the neutral. Since there is no formation of oxygen cluster anions, the possibility of electron transfer from excited Ti_8C_{12} to oxygen can be excluded. This could be possible only due to thermionic emission. During oxidation, neutral metcars reach highly excited states. Autoemission of electrons from these excited metcars results in the formation of metcar cations. This reaction gives an evidence for thermionic emission occurring in Ti_8C_{12}.

Dissociation dynamics

In order to provide evidence for the stability and structure of metcars, Castleman *et al.* conducted a systematic study of the collision-induced dissociation (CID) of $Ti_8C_{12}^+$ and related species under various collision conditions using a triple quadrupole mass spectrometer coupled with a laser vapourization source[65]. In collision-induced dissociation of $Ti_8C_{12}^+$ at a collision pressure of less than 0.1 mtorr, fragmentation occurs primarily due to single collision events, the primary product being $Ti_7C_{12}^+$, resulting from a loss of neutral titanium atom. The products $Ti_7C_{12}^+$, $Ti_6C_{12}^+$, $Ti_5C_{12}^+$ and Ti^+ result from both single and multiple collisions. The dissociation threshold of Ti_8C_{12} is found to be 9 eV, which indicates that it is a very stable cluster. Under high collision energy and high krypton pressure (Figure 6), no single carbon loss was observed for $Ti_8C_{12}^+$, but C_2 and C_3 units are lost, which suggests that C=C bonds are more important in both the formation and dissociation mechanisms of $Ti_8C_{12}^+$. Several larger $Ti_{9,10}C_y^+$ clusters are found to fragment to $Ti_8C_{12}^+$ by loss of metal–carbon units, which proves that $Ti_8C_{12}^+$ is unusually stable. The high dissociation threshold of $Ti_8C_{12}^+$, its fragmentation pattern and the fact that larger $Ti_{9,10}C_y^+$ clusters fragment to $Ti_8C_{12}^+$ provides evidence that metcars are quite stable, which is consistent with their proposed cage structure.

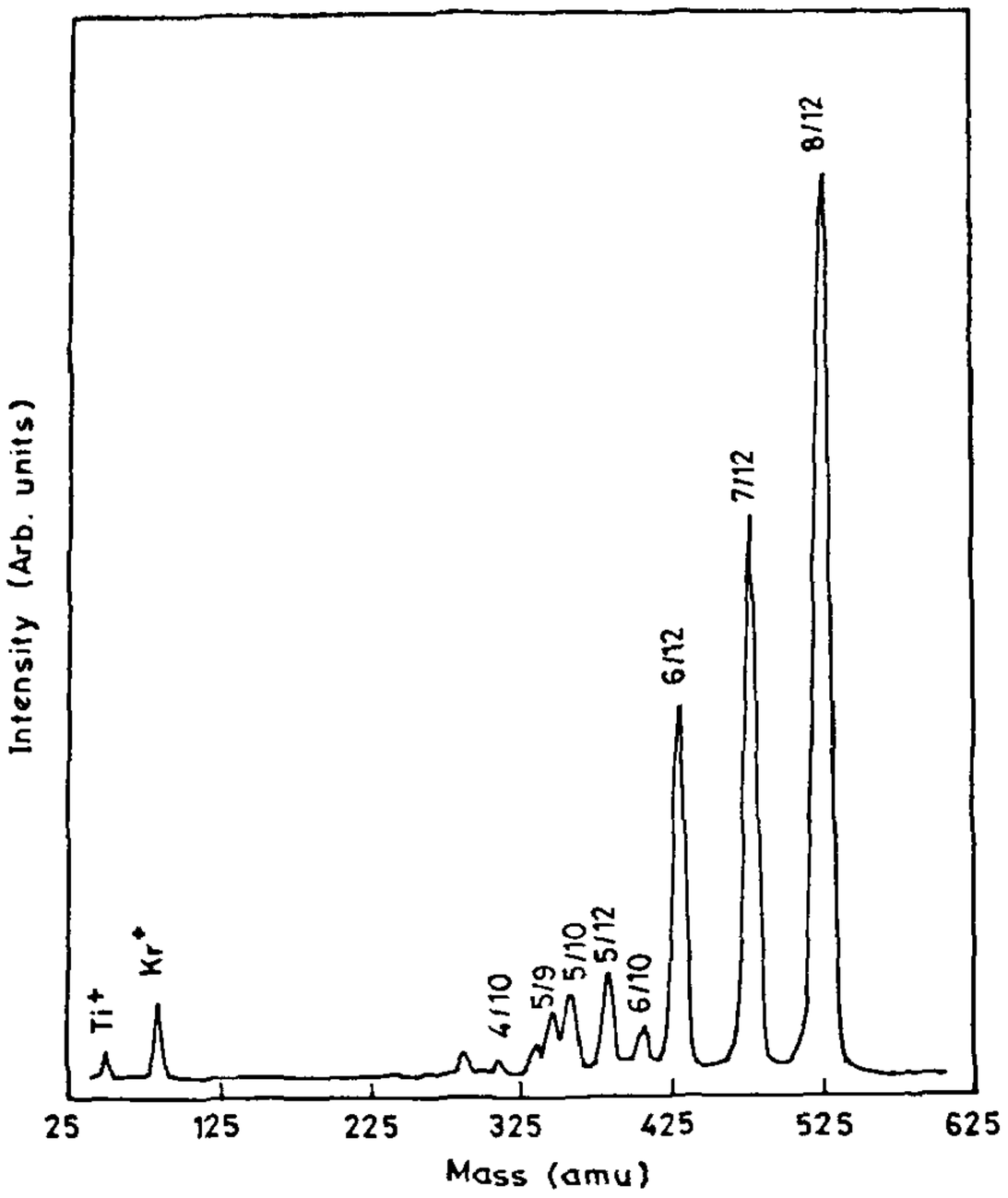

Figure 6. CID spectrum of $Ti_8C_{12}^+$ at high pressure (0.97 mtorr of He) and high collision energy (200 eV) (from ref. 65).

All the experimental work on metcars have been performed on the cations. Theoretical investigations have focused primarily on neutral clusters. Photoionization is the only way to probe neutral clusters in a molecular beam and such a study is interesting because it provides a comparison between neutral and cationic clusters. Ionization potentials from photoionization studies pro-

vide an indicator for the relative stability of corresponding neutral and cationic clusters. The distribution of neutral clusters is investigated by time of flight (TOF) mass spectrometry with photoionization at variety of laser wavelengths. The mass distribution for Ti/C clusters at three different laser powers (365, 44, and 5 $\mu J/cm^2$) was studied. All cluster masses observed are reduced in intensity as the laser power is reduced but relative intensities of these peaks are constant, suggesting that the clusters are not fragmented by multiphoton absorption. The intensities of these peaks vary linearly with laser power and the clusters represented by these mass peaks have ionization potentials lower than the laser photon energy of 5.76 eV. The power dependence of photoionization at 215 nm for Zr_8C_{12} and V_8C_{12} clusters[66] was studied and in both systems, photoionization was studied down to the $\mu j/pulse.cm^2$ energy domain, and slopes of the log(intensity)–log(laser power) plots were greater than two, indicating an ionization process due to two photon ionization[66]. These studies indicate[66] that $Zr_8C_{12}^+$, $V_8C_{12}^+$, etc. have ionization potentials in excess of 5.76 eV.

For Ti_8C_{12}, laser power dependence was studied in the region of 4.5–5.7 eV photon energy[66]. At 215 nm (5.76 eV) the power dependence is linear, which is consistent with one photon process. At low energies, power dependence changes to quadratic, which suggests a two-photon process. Figure 7 shows laser power dependence near 4.9 eV where log–log plots show a gradual change from linear to quadratic at 4.9 ± 0.2 eV, which is considered as the transition region. This is the transition point representing the threshold for one photon ionization. The ionization potential measured this way is the vertical ionization potential[66]. Calculated ionization potential for T_h symmetry is 6.0–6.9 eV and for T_d symmetry it is 4.5–3.7 eV.

In photoionization experiments, Ti_8C_{12} peak is not present with enhanced abundance because this cluster is not present as a super-abundant neutral; as a cation $Ti_8C_{12}^+$ is superabundant, which is surprising. Another interesting result from these ionization experiments is the absence of $M_{14}C_{13}^+$ cluster mass. Both Ti_8C_{12} and $Ti_{14}C_{13}$ have enhanced stability as cations but not as neutrals. Possibly, the missing magic number neutrals may be due to near-threshold ionization, the low excess energy in this kind of ionization might lead to a pronounced time delay effect, which could consequently result in a low intensity in the appropriate mass channel. The observation of delayed thermionic emission in multiphoton ionization of Ti_8C_{12} does suggest such a possibility (see below). Photodissociation of binary metal metallocarbohedrenes has also been investigated by a new technique (see ref. 67). The results emphasize the fact that the dominant mechanism proceeds through the loss of neutral titanium atoms for all clusters studied.

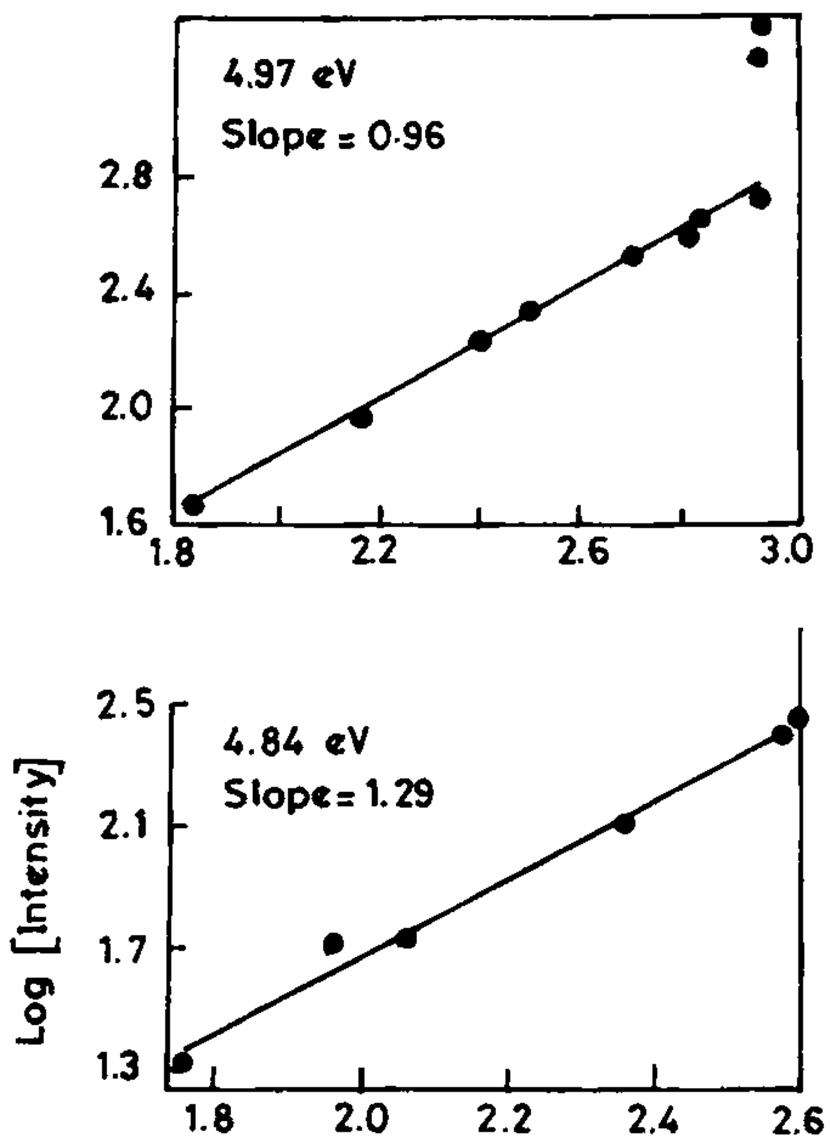

Figure 7. Power dependence studies of Ti_8C_{12} photoionization in the limit of low laser power. The photon order changes from a two photon process at lower energy to a one photon process at higher energy (from ref. 66).

Experimental electronic structure

To find whether metallocarbohedrenes have unusual electronic behaviour due to collective effects, Castleman *et al.* undertook a study of their potential for undergoing presence of delayed single atomic ion emission for metcar clusters arising from the excitation of collective giant dipole resonances in the system. For a cluster to undergo thermionic emission, the ionization potential must be at or below the dissociation energy for competition between the two processes, which results in delayed electron emission[68].

The metcars studied in these experiments were prepared in a standard laser vapourization source and were then directed into the reflectron TOFMS. Prompt ions which arise as a result of multiphoton ionization are

eliminated by modification in the ionization lens assembly. The characteristic times describing the experiment are: t_0, time zero for the experiment when the excitation laser fires; t_b, duration of the blocking field; t_e, time following excitation when the extraction field is switched on and; $t_e - t_b$, duration of field free time window.

Typical time scales for these experiments are $0\ \mu s \leq t_b \leq 2\ \mu s$ and $2\ \mu s \leq t_e \leq 3\ \mu s$. Use of the blocking field eliminates the possibility that field-induced ionization of states lying close to ionization threshold contribute to the observed delayed ion signal. Mass spectra obtained with $t_b = 1.5\ \mu s$ to block all prompt ions with masses up to 700 amu show only delayed ion peaks corresponding to metcar and atomic metal ion. Among various metal carbon species, only M_8C_{12} exhibits delayed ionization behaviour, which reinforces the point that it has a special structure and unique properties. The peaks which are appearing at the single atomic mass and at the metcar mass region arise from ionization occurring in field free time window after the blocking field is turned to zero and before the extraction field is turned on. Thus two ionization channels are active, one leading to the formation of $M_8C_{12}^+$ and the other resulting in M^+. When $t_b = 0.5\ \mu s$, the M^+ region consists of two peaks, of which one is the promptly ionized M^+ and other M^+ arising from delayed ionization/fragmentation. As t_b is scanned from 0.0 to 2.0 μs, intensity maximum of the peak shifts from left-most values of t_b to right-most values. (Figure 8). If clustering conditions in the source are changed to minimize the presence of large clusters, the two peaks collapse into a single peak at which no delayed ionization occurs. Therefore, delayed ionization occurs due to heavier clusters[62].

At excitation wavelengths of 355 nm (3.49 eV) and 532 nm (2.33 eV), the metcar cluster ions formed by prompt or delayed ionizations must be the result of multiphoton process as the IP of metcar is ~5 eV (ref. 66). Delayed ionization channel is active at lower laser fluence which results in the production of $M_8C_{12}^+$. $M_8C_{12}^+$ begins to plateau as fluence is increased and delayed M^+ peak begins to appear. Therefore, M^+ results from fragmentation of excited larger clusters.

The fluence dependence of delayed ions was studied at both 355 nm and 532 nm. Ionization behaviour was observed to be similar at the two different wavelengths[68]. This suggests that there is no particular excited state which plays a distinct role in delayed ionization, but large number of closely-spaced excited states allow photons of both wavelengths to contribute to the excitation. This demonstrates the existence of thermionic emission, larger number of closely-spaced states forming a heat bath which allows the cluster to store the excitation energy.

During the absorption of at least two photons, electronically excited M_8C_{12} nonradiatively decays, leading to the population of many closely-spaced states, which further leads to the formation of electronically and vibrationally excited clusters. Delayed ionization results from a slow coupling of excited electronic and vibrational states. Hence delayed $M_8C_{12}^+$ signal is observed up to several microseconds following laser excitation of neutrals. Once the vibrationally/electronically excited species populate the manifold states, subsequent absorption of photons can also occur. Absorption of two more photons at 355 nm produces excited species which have energies within the limits of predicted broad dipole resonance. Once this collective resonance has been accessed, energy redistribution results in delayed appearance of $Ti_8C_{12}^+$ or Ti^+ fragment.

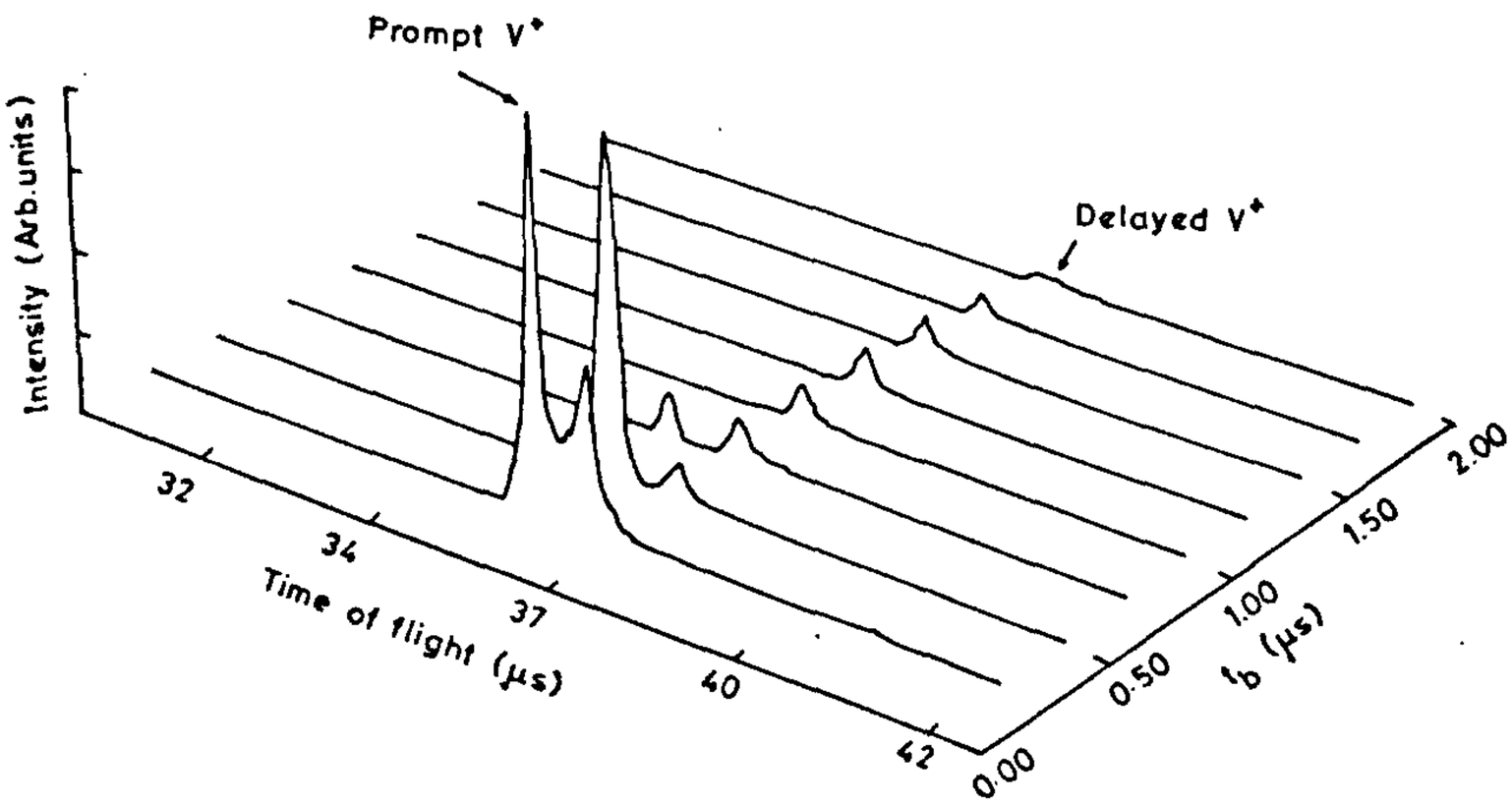

Figure 8. Intensities of prompt and delayed V^+. As t_b is scanned from 0.0 to 2.0 μs, the intensity maximum shifts from prompt V^+ to delayed V^+ (from ref. 68).

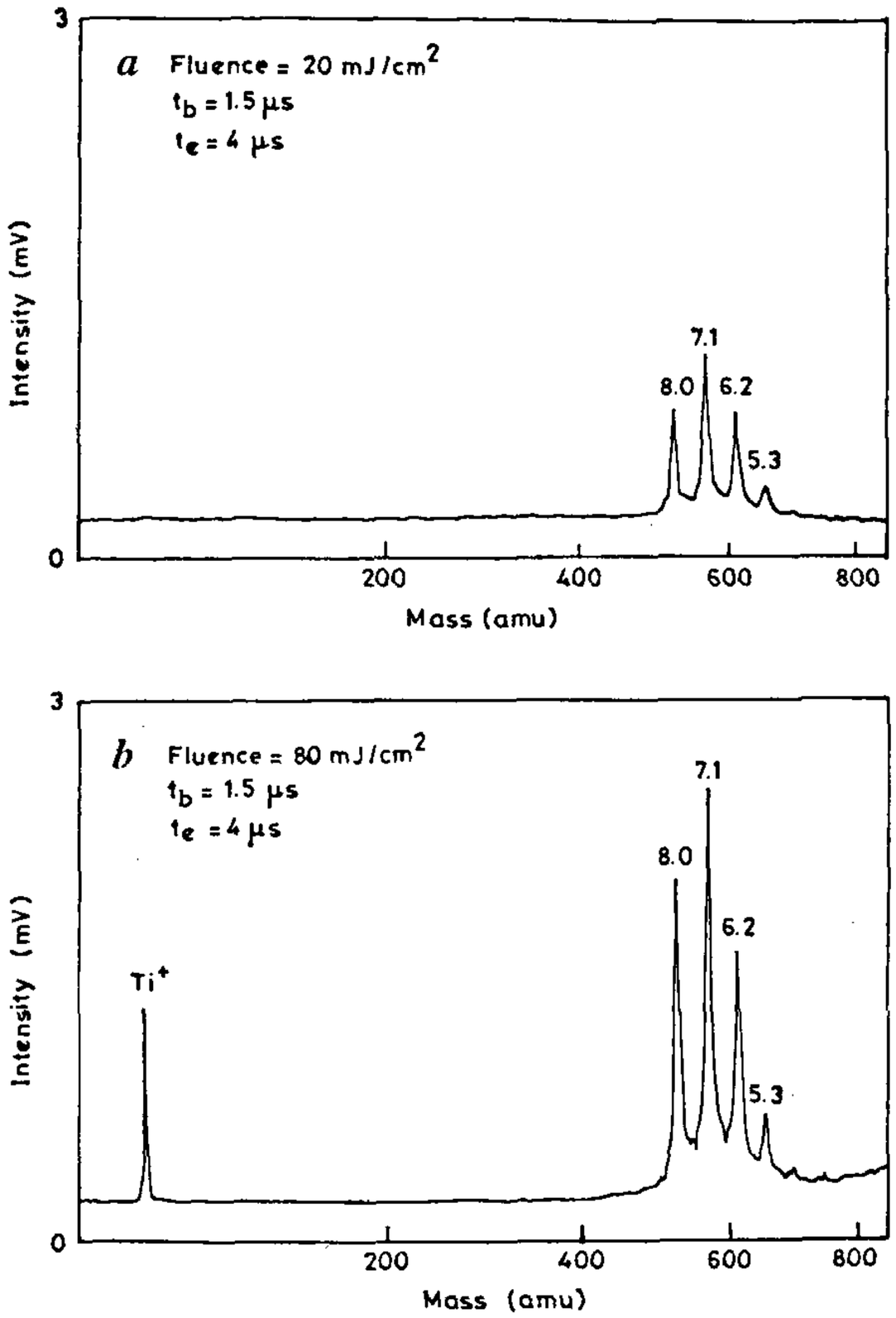

Figure 9. *a*, Mass spectrum of delayed $Ti_xZr_yC_{12}$ clusters at lower laser fluence (20 mJ/cm^2); *b*, mass spectrum of delayed Ti^+ and $Ti_xZr_yC_{12}$ clusters under higher fluence (80 mJ/cm^2) (from ref. 69).

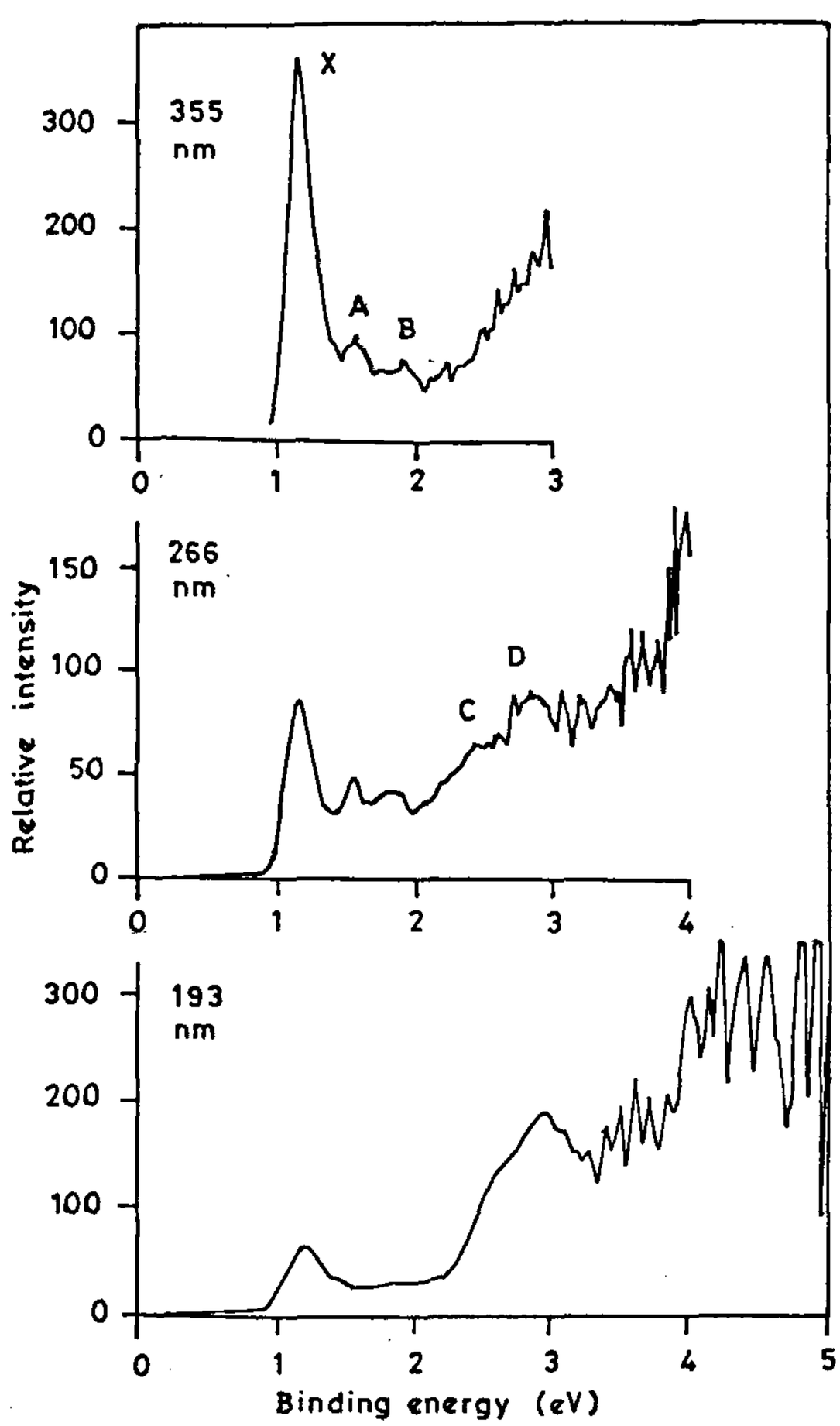

Figure 10. Photoelectron spectra of $Ti_8C_{12}^+$ at three different photon energies: 355 nm (3.49 eV), 266 nm (4.66 eV), and 193 nm (6.42 eV) (from ref. 70).

Investigations of the photophysical character of binary metal containing metallocabohedrene clusters suggest that they also exhibit the phenomenon of delayed ionization. Binary metal metcars of Ti with Zr or Nb were studied for this purpose. Here time-dependent yield of delayed ion signal was found along with delayed metal ion production. To verify whether the atomic ion signal was due to a delayed ion, its intensity was monitored as a function of various delay times. From these studies it was concluded that Ti^+ is the result of emission from an excited metcar species[69].

The time-dependent yield of delayed ionization and atomic ion emission was observed by setting extraction voltage pulse at $t_e = 3$ μs. From the plot of ion signal intensity versus t_0 for Ti_8C_{12}, $Ti_7Nb_3C_{12}$ and $Ti_5Nb_3C_{12}$, it was found that pure Ti_8C_{12} displays slower decay than binary metals species. As degree of substitution is reduced, life-time of neutral metcar is increased. At $t_e = 3$ μs and $t_b = 1.5$ μs, ionization laser power was varied at 532, 355 and 266 nm to study the wavelength and fluence dependence of delayed ion formation processes. Observation of delayed ionization for three different wavelengths provides further evidence that no specific excited electronic state is involved in the ionization process. As power is decreased (from 80 mJ/cm^2 to 20 mJ/cm^2 at 355 nm), delayed ion signal decreases and delayed Ti^+ disappears (Figure 9). As fluence is decreased, only delayed ionization channel is observed. At a particular threshold fluence (at 25 mJ/cm^2), Ti^+ disappears which suggests that several channels are active at higher fluence. At higher fluences, vibronically excited neutral species (delayed ion precursors) absorb more photons. Absorption of two more photons at 355 nm or three photons at 532 nm produces excited

state species having energies within the limits of collective resonance of metcar species (excited neutrals or ions) which emit the atomic ion.

The degree of delayed ionization relative to the total ionization yield is obtained from the plot of ratios of delayed ion vs total ion signal intensities. The higher energy collective resonance is not found under low fluence conditions and the competitive channel resulting in atomic ion emission is not observed. When $t_b = 0$ μs, metcar ion signal is due to both delayed ion and prompt ions. At $t_b = 1.6$ μs, all ions are only due to delayed ions since prompt ions are eliminated. From the ratio of delayed ion signal (I_d) at $t_b = 1.6$ μs to total ion signal ($I_d + I_p$) at $t_b = 0$ μs, we can find the degree of delayed ionization.

Photoelectron spectroscopic (PES) studies have been performed on metallocarbohedrene $Ti_8C_{12}^-$ to obtain the electronic structure information[70]. The $Ti_8C_{12}^-$ clusters were produced by laser vapourization of a solid TiC target with neat He carrier gas. At two different photon energies, 3.49 and 4.66 eV, photoelectron spectra were obtained for all mass channels from TiC_4^- to $Ti_9C_y^-$. The $Ti_8C_{12}^-$ spectrum is special with an intense threshold peak, from which the electron affinity (EA) of Ti_8C_{12} obtained to be 1.05 ± 0.05 (adiabatic) and 1.16 ± 0.05 eV (vertical). Ti_8C_{12} has a lowest EA among all the species. Low-electron affinity for Ti_8C_{12} is responsible for low mass abundance of $Ti_8C_{12}^-$. PES of $Ti_8C_{12}^-$ at three different photon energies are shown in Figure 10. Three features X (1.16 eV), A (1.56 eV) and B (1.81 eV) are clearly observed at 3.49 eV spectrum. Signals at higher binding energies are also observed at C (2.5 eV) and D (2.9 eV). Two sets of features are observed in 6.42 eV spectrum. The low-energy features (X, A and B) are followed by a small energy gap (0.7 eV) and then higher energy features (C and D) are seen. Ti_8C_{12} consists of 32 valence electrons on Ti atoms in which only 20 electrons are available for metal–metal interactions (12 are donated to six C_2 units). There are two extra electrons in addition to the stable 18 electron structure to make Ti_8C_{12} a 20 electron system. The two extra electrons occupy the higher energy $2a_1$ orbital (in the T_d structure) and this explains the low ionization potential measured for Ti_8C_{12}, since $2a_1$ electrons are expected to be easily ionized.

The orbital diagram shown in Figure 11 explains the photoelectron spectrum. The extra electron enters the $2t_2$ orbital of the anion. Since $2t_2$ orbital is high in energy, a low-electron affinity is understandable. The occupation of the $2t_2$ orbital results in a degenerate ground state for $Ti_8C_{12}^-$. Removal of electron from $2t_2$ orbital leads to the PES feature (X). The width of this feature suggests a Jahn–Teller effect resulting from the change of the anion to the neutral transition. Removal of $2a_1$ electron results in two low-lying states (A and B) because of singlet-triplet coupling. Removal of spin-up $2a_1$ electron yields feature A (likely to be singlet state), while feature B (the triplet state) arises due to removal of the spin-down $2a_1$ electron. A–B energy separation yields a singlet–triplet coupling energy of 0.25 eV. After an energy gap of 0.7 eV, the features C and D seen in the spectrum are due to the removal of electrons from highest bonding orbital $1t_1$. Removal of electrons from other bonding orbitals results in higher energy features as seen in the 6.42 eV spectrum. Features A and B have low intensities since their orbital origin ($2a_1$) is nondegenerate. Apart from explaining the experimental observations such as low IP (high cation abundance), chemisorption of four π-bonding molecules, low EA (low abundance of anion) and halogen abstraction reaction, the electronic structure of T_d Ti_8C_{12} provides a detailed interpretation of the PES spectrum.

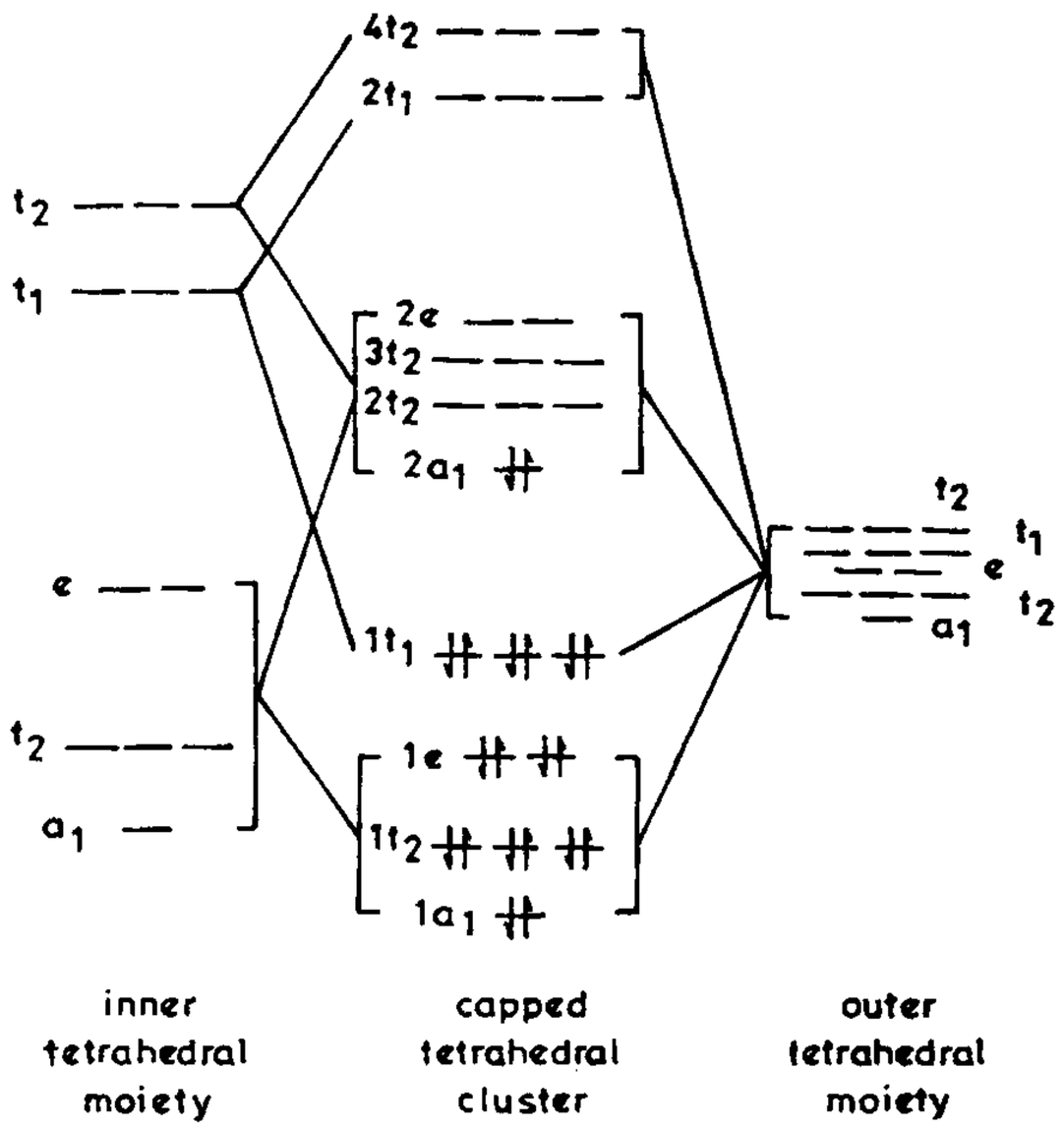

Figure 11. Orbital diagram showing the valence molecular orbitals resulting from the metal–metal interactions for a tetracapped Ti_8C_{12} met-car (from ref. 18).

Important properties of metcars derived from experiments are given in Table1.

Perspectives

Although many of the properties of metcars are known, they still remain elusive; probed only by the most advanced tools of gas phase spectroscopy. Nearly all of the available experimental information is on metcar ions and there are indeed substantial variations in the chemistry of different metcar ions. Many of the fundamental

Table 1. Summary of important experiments done on $Ti_8C_{12}^+$

Experiment done on $Ti_8C_{12}^+$	Properties studied
Ion chromatography	Ionic mobility = 5.78 $cm^2V^{-1}s^{-1}$ (experimental) Ionic mobility = 5.71 $cm^2V^{-1}s^{-1}$ (calculated)
Collision-induced dissociation	Dissociation threshold = 70 eV at a centre of mass energy of 9 eV.
Near threshold photoionization	Ionization potential = 4.9 ± 0.2 eV (experimental) Calculated ionization potential for T_h structure = 6.05 eV, 5.33 eV, and 5.4 eV. T_d structure = 6.82 eV, 4.5 eV, 4.37 eV and 6.74 eV. D_{2d} structure = 5.8 eV.
Photoelectron spectroscopy	Electron affinity = 1.05(± 0.05 eV) (adiabatic) Electron affinity = 1.16(± 0.05 eV) (vertical)
Reaction of Ti–C clusters	Differences in reactivity of $Ti_8C_{12}^+$ and other Ti–C clusters ($Ti_8C_{11}^+$, $Ti_8C_{13}^+$)
Studies of metcar adducts (Reaction of metcar with halogens, π-bonding molecules, and polar molecules)	Reaction mechanisms of $Ti_8C_{12}^+$ are identified and characterized namely oxidation, complexation and ion dipole interaction and evidence for T_h structure is obtained.
FT–ICR Studies for reaction of $V_8C_{12}^+$ with H_2O, NH_3, CH_3OH and CH_3X (X = Cl, Br and I)	Provide evidence for T_d or D_{2d} symmetry of $V_8C_{12}^+$.
Investigations of the ionization channels of titanium and vanadium carbon clusters	Supports the mechanism of thermionic emission and delayed single atomic ion emission from metcar clusters.

properties of metcars are still not known, computations offer no great help in view of the complexity of these systems. An efficient way of synthesizing metcars in the solid state is eagerly awaited. The spectroscopy, electronic, magnetic and catalytic properties of metcars will indeed be fascinating which will make this area important in the years to come.

1. Castleman, Jr. A. W. and Keese, R. G., *Science*, 1988, **241**, 36–42.
2. Kroto, H. W., Heath, J. R., O'Brien, S. C., Curl, R. F. and Smalley, R. E., *Nature*, 1985, **318**, 162–163.
3. Guo, B. C., Kerns, K. P. and Castleman, Jr. A. W., *Science*, 1992, **255**, 1411–1413.
4. Guo, B. C., Wei, S., Purnell, J., Buzza, S. and Castleman, Jr. A. W., *Science*, 1992, **256**, 515–516.
5. Wei, S., Guo, B. C., Purnell, J., Buzza, S. and Castleman, Jr. A. W., *Science*, 1992, **256**, 818–820.
6. Pilgrim, J. S. and Duncan, M. A., *J. Am. Chem. Soc.*, 1993, **115**, 4395–4396.
7. Wei, S., Guo, B. C., Deng, H. T., Kerns, K., Purnell, J., Buzza, S. A. and Castleman, Jr. A. W., *J. Am. Chem. Soc.*, 1994, **116**, 4475–4476.
8. Purnell, J., Wei, S. and Castleman, Jr. A. W., *Chem. Phys. Lett.*, 1994, **229**, 105– 110.
9. Pilgrim, J. S. and Duncan, M. A., *J. Am. Chem. Soc.*, 1993, **115**, 6958–6961.
10. Pilgrim, J. S., Brock, L. R. and Duncan, M. H., *J. Phys. Chem.*, 1995, **99**, 544–550.
11. Cartier S. F., May, B. D. and Castleman, Jr. A. W., *J. Am. Chem. Soc.*, 1994, **116**, 5295–5297.
12. Wei, S., Guo, B. C., Purnell, J., Buzza, S. and Castleman, Jr. A. W., *J. Phys. Chem.*, 1992, **96**, 4166–4168.
13. Wei, S., Guo, B. C., Purnell, J., Buzza, S. and Castleman, Jr. A. W., *J. Phys. Chem.*, 1993, **97**, 9559–9561.
14. Guo, B. C., Kerns, K. P. and Castleman, Jr. A. W., *J. Am. Chem. Soc.*, 1993, **115**, 7415–7418.
15. Deng, H. T., Guo, B. C. and Castleman, Jr. A. W., *J. Phys. Chem.*, 1994, **98**, 13373– 13378.
16. Pradeep, T. and Manoharan, P. T., *Curr. Sci.*, 1995, **68**, 1017–1026.
17. Lin, Z. and Hall, M. B., *J. Am. Chem. Soc.*, 1992, **114**, 10054–10055.
18. Lin, Z. and Hall, M. B., *J. Am. Chem. Soc.*, 1993, **115**, 11165–11168.
19. Grimes, R. W. and Gale, J. D., *J. Chem. Soc. Chem. Commun.*, 1992, 1222–1224.
20. Grimes, R. W. and Gale, J. D., *J. Chem. Soc., J. Phys. Chem.*, 1993, **97**, 4616–4620.
21. Pauling, L., *Proc. Natl. Acad. Sci. USA*, 1992, **89**, 8125.
22. Reddy, B. V., Khanna, S. N. and Jena, P., *Science*, 1992, **258**, 1640–1643.
23. Lou, L., Guo, T., Nordlander, P. and Smalley, R. E., *J. Chem. Phys.*, 1993, **99**, 5301–5305.
24. Methfessel, M., Van Schilfgaarde, M. and Scheffler, M., *Phys. Rev. Lett.*, 1993, **70**, 29–32.
25. Methfessel, M, Van Schilfgaarde, M. and Scheffler, M., *Phys. Rev. Lett.*, 1993, **71**, 209.
26. Reddy, B. V. and Khanna, S. N., *Chem. Phys. Lett.*, 1996, **100**, 19211–19214.

27. Reddy, B. V. and Khanna, S. N., *J. Phys. Chem.*, 1994, **98**, 9446–9449.
28. Lou, L. and Nordlander, P., *Chem. Phys. Lett.*, 1994, **224**, 439–444.
29. Naga Srinivas, G., Srinivas, H. and Jemmis, E. D., *Proc. Indian Acad. Sci. (Chem. Sci.)*, 1994, **106**, 169–181.
30. Rubio, A., Alonso, J. A. and Lopez, J. M., *An. Fis.*, 1993, **89**, 174–179.
31. Hay, P. J., *J. Phys. Chem.*, 1993, **97**, 3081–3083.
32. Chen, H., Feyereisen, M., Long, X. P. and Fitzgerald, G., *Phys. Rev. Lett.*, 1993, **71**, 1732–1735.
33. Cuelemans, A. and Fowler, P. W., *J. Chem. Soc. Faraday Trans.*, 1992, **88**, 2797–2798.
34. Rohmer, M., de Vaal, P. and Benard, M., *J. Am. Chem. Soc.*, 1992, **114**, 9696–9697.
35. Dance, I., *J. Chem. Soc. Chem. Commun.*, 1992, 1779–1780.
36. Rohmer, M., Benard, M., Henriet, C., Bo, C. and Poblet, J. M., *J. Chem. Soc. Chem. Commun.*, 1993, 1182–1185.
37. Dance, I., *J. Am. Chem. Soc.*, 1996, **118**, 2699–2707.
38. Rohmer, M., Benard, M., Bo, C. and Poblet. J., *J. Am. Chem. Soc.*, 1995, **117**, 508–517.
39. Rohmer, M., Benard. M., Bo, C. and Poblet. J., *J. Phys. Chem.*, 1995, **99**, 16913–16924.
40. Dance, I., *J. Am. Chem. Soc.*, 1996, **118**, 6309–6310.
41. Von Helden, G., Hsu, M-T., Gotts, N. and Bowers, M. T., *J. Phys. Chem.*, 1993, **97**, 8182–8184.
42. Cartier, S. F., May, B. D., Toleno, B. J., Purnell, J., Wei, S. and Castleman, Jr. A. W., *Chem. Phys. Lett.*, 1994, **220**, 23–28.
43. Chen, Y., Walder, G. J. and Castleman, Jr. A. W., *J. Phys. Chem.*, 1992, **96**, 9581–9582.
44. Cartier, S. F., Chen, Z. Y., Walder, G. J., Sleppy, G. R. and Castleman, Jr. A. W., *Science*, 1993, **260**, 195–196.
45. Lu, W., Huang, R., Ding, J. and Yang, S., *J. Chem. Phys.*, 1996, **104**, 6577–6581.
46. Tast, F., Malinowski, N., Frank, S., Heinebrodt, M. and Bilas, I. M. L., *Phys. Rev. Lett.*, 1996, **77**, 3529–3532.
47. Khan, A., *Chem. Phys. Lett.*, 1995, **247**, 447–453.
48. Pilgrim, J. S. and Duncan, M. A., *J. Am. Chem. Soc.*, 1993, **115**, 9724–9727.
49. Pilgrim, J. S. and Duncan, M. A., *Int. J. Mass Spectrum. Ion Processes*, 1994, **138**, 283.
50. Khan, A., *J. Phys. Chem.*, 1995, **99**, 4923–4928.
51. Khan, A., *J. Phys. Chem.*, 1993, **97**, 10937–10938.
52. Poblet, J. M., Bo, C., Rohmer, M-M. and Benard, M., *Chem. Phys. Lett.*, 1996, **260**, 577–581.
53. Khanna, S. N., *Phys. Rev. B.*, 1995, **51**, 10965–10967.
54. Kerns, K. P., Guo, B. C., Deng, H. T. and Castleman, Jr. A. W., *J. Am. Chem. Soc.*, 1995, **117**, 4026–4029.
55. Deng, H. T., Kerns, K. P. and Castleman, Jr. A. W., *J. Am. Chem. Soc.*, 1996, **118**, 446–450.
56. Yeh, C. S., Afzaal, S., Lee, S. A., Byun, Y. G. and Freiser, B. S., *J. Am. Chem. Soc.*, 1994, **116**, 8806–8807.
57. Byun, Y. G. and Freiser, B. S., *J. Am. Chem. Soc.*, 1996, **118**, 3681–3686.
58. Byun, Y. G., Yeh, C. S., Xu, Y. C. and Freiser, B. S., *J. Am. Chem. Soc.*, 1995, **117**, 8299–8303.
59. Byun, Y. G., Lee, S. A., Kan, S. Z. and Freiser, B. S., *J. Phys. Chem.*, 1996, **100**, 14281–14288.
60. Bowers, M. T., Kemper, P. R., Helden, G. V. and Van Koppen, P. A. M., *Science*, 1993, **260**, 1446–1451.
61. Bowers, M. T., *Acc. Chem. Res.*, 1994, **27**, 324–332.
62. Lee, S., Gotts, N. G., Helden, J. V. and Bowers, M. T., *Science*, 1995, **267**, 999–1001.
63. Cartier, S. F., May, B. D. and Castleman, Jr. A. W., *J. Phys. Chem.*, 1996, **100**, 8175–8179.
64. Deng, H. T., Kerns, K. P. and Castleman, Jr. A. W., *J. Chem. Phys.*, 1996, **104**, 4862– 4864.
65. Kerns, K. P., Guo, B. C., Deng, H. T. and Castleman, Jr. A. W., *J. Chem. Phys.*, 1994, **101**, 8529–8534.
66. Brock, L. R. and Duncan, M. A., *J. Phys. Chem.*, 1996, **100**, 5654–5659.
67. May, B. D., Kooi, S. E., Toleno, B. J. and Castleman, Jr. A. W., *J. Chem. Phys.* 1997, **106**, 2231–2238.
68. May, B. D., Cartier, S. F. and Castleman, Jr. A. W., *Chem. Phys. Lett.*, 1995, **242**, 265–272.
69. Cartier, S. F., May, D. and Castleman, Jr. A. W., *J. Chem. Phys.*, 1996, **104**, 3423–3432.
70. Wang, L-S., Li, S. and Wu, H., *J. Phys. Chem.*, 1996, **100**, 19211–19214.

ACKNOWLEDGEMENTS. We acknowledge financial support from the Department of Science and Techonology, Government of India through a research grant awarded to T. Pradeep and P. T. Manoharan.

Received 11 November 1997; accepted 12 February 1998.